Differential effects of cisplatin on cybrid cells with varying mitochondrial DNA haplogroups

Sina Abedi [Corresp., 1], **Gregory Yung** [1], **Shari R Atilano** [1], **Kunal Thaker** [1], **Steven Chang** [1], **Marilyn Chwa** [1], **Kevin Schneider** [1], **Nitin Udar** [1], **Daniela Bota** [2], **M Cristina Kenney** [Corresp. 1, 3]

[1] Gavin Herbert Eye Institute, University of California, Irvine, Irvine, CA, United States

[2] Department of Neurology, Neuro-Oncology Division, University of California, Irvine, Irvine, CA, United States

[3] Department of Pathology and Laboratory Medicine, University of California, Irvine, Irvine, CA, United States

Corresponding Authors: Sina Abedi, M Cristina Kenney
Email address: sabedi1@uci.edu, mkenney@hs.uci.edu

Background. Drug therapy yields different results depending on its recipient population. Cisplatin, a commonly used chemotherapeutic agent, causes different levels of resistance and side effects for different patients, but the mechanism(s) are presently unknown. It has been assumed that this variation is a consequence of differences in nuclear (n) DNA, epigenetics, or some external factor(s). There is accumulating evidence that an individual's mitochondrial (mt) DNA may play a role in their response to medications. Variations within mtDNA can be observed, and an individual's mtDNA can be categorized into haplogroups that are defined by accumulations of single nucleotide polymorphisms (SNPs) representing different ethnic populations.

Methods. The present study was conducted on transmitochondrial cytoplasmic hybrids (cybrids) that possess different maternal-origin haplogroup mtDNA from African (L), Hispanic [A+B], or Asian (D) backgrounds. Cybrids were created by fusing Rho0 ARPE-19 cells (lacking mtDNA) with platelets, which contain numerous mitochondria but no nuclei. These cybrid cells were cultured to passage five, treated with cisplatin, incubated for 48h, then analyzed for cell metabolic activity (tetrazolium dye (MTT) assay), mitochondrial membrane potential (JC-1 assay), cytotoxicity (lactate dehydrogenase (LDH) assay), and gene expression levels for *ALK*, *BRCA1*, *EGFR*, and *ERBB2/HER2*.

Results. Results indicated that untreated cybrids with varying mtDNA haplogroups had similar relative metabolic activity before cisplatin treatment. When treated with cisplatin, (1) the decline in metabolic activity was greatest in L (27.4%, $p < 0.012$) > D (24.86%, $p = 0.0001$) and [A+B] cybrids (24.67%, $p = 0.0285$) compared to untreated cybrids; (2) mitochondrial membrane potential remained unchanged in all cybrids (3) LDH production varied between cybrids (L > [A+B], $p = 0.0270$). (4) The expression levels decreased for *ALK* in L ($p < 0.0001$) and [A+B] ($p = 0.0001$) cybrids but not in D cybrids ($p = 0.285$); and decreased for *EGFR* in [A+B] cybrids ($p = 0.0246$) compared to untreated hybrids.

Conclusion. Our findings suggest that an individual's mtDNA background may be associated with variations in their response to cisplatin treatment, thereby affecting the efficiency and the severity of side effects from the treatment.

Differential effects of cisplatin on cybrid cells with varying mitochondrial DNA haplogroups

Sina Abedi[1], Gregory Yung[1], Shari R. Atilano[1], Kunal Thaker[1], Steven Chang[1], Marilyn Chwa[1], Kevin Schneider[1], Nitin Udar[1], Daniela Bota[2], M. Cristina Kenney[1, 3]

[1]Gavin Herbert Eye Institute, University of California Irvine, Irvine, CA, USA
[2]Department of Neurology, Neuro-Oncology Division, University of California Irvine, Irvine, CA, USA
[3]Department of Pathology and Laboratory Medicine, University of California Irvine, Irvine, CA, USA

Corresponding Authors:
M. Cristina Kenney, M.D., Ph.D.
Gavin Herbert Eye Institute, Ophthalmology Research Laboratory
University of California Irvine, Hewitt Hall, Room 2028
843 Health Science Road
Irvine, CA 92697
Email address: mkenney@hs.uci.edu

Sina Abedi
Gavin Herbert Eye Institute, Ophthalmology Research Laboratory
University of California Irvine, Hewitt Hall, Room 2028
843 Health Science Road
Irvine, CA 92697
Email address: sabedi1@uci.edu

Abstract

Background. Drug therapy yields different results depending on its recipient population. Cisplatin, a commonly used chemotherapeutic agent, causes different levels of resistance and side effects for different patients, but the mechanism(s) are presently unknown. It has been assumed that this variation is a consequence of differences in nuclear (n) DNA, epigenetics, or some external factor(s). There is accumulating evidence that an individual's mitochondrial (mt) DNA may play a role in their response to medications. Variations within mtDNA can be observed, and an individual's mtDNA can be categorized into haplogroups that are defined by accumulations of single nucleotide polymorphisms (SNPs) representing different ethnic populations.

Methods. The present study was conducted on transmitochondrial cytoplasmic hybrids (cybrids) that possess different maternal-origin haplogroup mtDNA from African (L), Hispanic [A+B], or Asian (D) backgrounds. Cybrids were created by fusing Rho0 ARPE-19 cells (lacking mtDNA) with platelets, which contain numerous mitochondria but no nuclei. These cybrid cells were cultured to passage five, treated with cisplatin, incubated for 48h, then analyzed for cell metabolic activity (tetrazolium dye (MTT) assay), mitochondrial membrane potential (JC-1 assay), cytotoxicity (lactate dehydrogenase (LDH) assay), and gene expression levels for *ALK*, *BRCA1*, *EGFR*, and *ERBB2/HER2*.

Results. Results indicated that untreated cybrids with varying mtDNA haplogroups had similar relative metabolic activity before cisplatin treatment. When treated with cisplatin, (1) the decline in metabolic activity was greatest in L (27.4%, $p < 0.012$) > D (24.86%, $p = 0.0001$) and [A+B] cybrids (24.67%, $p = 0.0285$) compared to untreated cybrids; (2) mitochondrial membrane potential remained unchanged in all cybrids (3) LDH production varied between cybrids (L > [A+B], $p = 0.0270$). (4) The expression levels decreased for *ALK* in L ($p < 0.0001$) and [A+B] ($p = 0.0001$) cybrids but not in D cybrids ($p = 0.285$); and decreased for *EGFR* in [A+B] cybrids ($p = 0.0246$) compared to untreated cybrids.

Conclusion. Our findings suggest that an individual's mtDNA background may be associated with variations in their response to cisplatin treatment, thereby affecting the efficiency and the severity of side effects from the treatment.

Introduction

Cisplatin is a platinum complex used in the chemotherapeutic treatments of various cancers, including ovarian and testicular cancers. It functions primarily by forming intrastrand crosslink adducts with the cell's DNA. This activates signal transduction pathways that disrupt transcription and replication, therefore inducing apoptosis in target cells (Dasari & Tchounwou 2014; Florea & Büsselberg 2011; Meijera et al. 2001; Siddik 2003). Side effects of cisplatin treatment include nausea, vomiting, hearing loss, myelosuppression, neurotoxicity, nephrotoxicity, hepatotoxicity, and cardiotoxicity (Dasari & Tchounwou 2014). Unfortunately, cisplatin resistance is common, and the biochemical mechanisms leading to resistance are only partially understood (Amable 2016; Boulikas & Vougiouka 2004; Cocetta et al. 2019; Damia &

Broggini 2019; Florea & Büsselberg 2011; Gottesman et al. 2016; Siddik 2003). Studies have shown that mechanisms related to DNA repair, decreased drug uptake, or decreased DNA adduct formation have been associated with increased cisplatin resistance (Amable 2016; Damia & Broggini 2019; Siddik 2003).

Variations in chemosensitivity to cisplatin have been observed in individuals of varying ethnic backgrounds (Jing et al. 2014; Kenney et al. 2014b; O'Donnell & Dolan 2009; Tan et al. 2016; Yasuda et al. 2008). In a study investigating genetic biomarkers, Caucasian individuals demonstrated significantly greater susceptibility to identical doses of cisplatin compared to Asian individuals with late-stage non-small lung cancer (NSCLC) (Rose et al. 2014). O'Donnell *et al.* found that individuals of Asian descent (excluding India) were more susceptible to chemotherapy agents than individuals of European descent, and additionally, individuals of African descent showed greater resistance to anticancer treatments than those of European descent (O'Donnell & Dolan 2009). These differences have previously been attributed to differences within the nuclear DNA and epigenetic factors (Amable 2016; Ha et al. 2018; Housman et al. 2014; O'Byrne et al. 2011; Siddik 2003; Stewart 2007; Ziliak et al. 2012).

Currently, evidence demonstrates that the mitochondria may also affect an individual's response to cisplatin treatment (Han et al. 2017; Marrache et al. 2014; Marullo et al. 2013; Tsuyoshi et al. 2017). Mitochondria are organelles that play an important role in ATP production, calcium homeostasis, cell signaling, and apoptosis. Previous studies have indicated that cisplatin treatment results in mitochondrial damage leading to reduced energy production and increased apoptotic activity (Devarajan et al. 2002; Han et al. 2017; Park et al. 2002; Patel et al. 2019; Tsuyoshi et al. 2017; Yáñez et al. 2003). Mitochondria are unique in that they contain their own DNA. Mitochondrial (mt) DNA is maternally inherited and can be categorized into haplogroups that are defined by single nucleotide polymorphism (SNP) variants. Different mtDNA haplogroups are used to classify populations of different maternal ancestral origins (www.mitomap.org/foswiki/pub/MITOMAP/MitomapFigures/WorldMigrations2012.pdf). Over the span of thousands of years, the different ancestral populations have accumulated distinct patterns of SNP variants within the mitochondrial genome, and it is likely that these SNP variants contribute to changes in cellular functions (Atilano et al. 2015; Jing et al. 2014; Kenney et al. 2014a; Kenney et al. 2014b; Kenney et al. 2013; Marrache et al. 2014; O'Donnell & Dolan 2009; Patel et al. 2019; Penta et al. 2001; Singh et al. 1999; Tan et al. 2016; van Gisbergen et al. 2015).

Damage to the mtDNA accumulates because mitochondria, unlike the nucleus, lack efficient DNA repair mechanisms. Germline and somatic mutations, as well as copy number differences within the mtDNA, are associated with increased cancer risk. These mutations are likely to remain within the genome and be passed on to offspring (van Gisbergen et al. 2015). Cisplatin susceptibility within the mitochondria could, however, be lessened. Variations within the

mtDNA that prevent cisplatin from affecting ATP production, altering signaling pathways, or forming DNA adducts could lead to cisplatin resistance (Czarnecka & Bartnik 2011; Florea & Büsselberg 2011; Jarrett et al. 2008; Kenney et al. 2014b; Kenney et al. 2013; Singh et al. 1999). Similarly, in a study on pancreatic cancer cells, Mizutani *et al.* demonstrated that mutations within the mitochondrial genome could result in cell resistance to cisplatin (Mizutani et al. 2009).

In order to study the effect(s) of differing mtDNA variants on drug susceptibility, the cybrid model can be used. Cybrids are transmitochondrial cell lines that contain identical nuclei, but mtDNA from different patients. These cybrids vary only in their mtDNA; therefore, differences in cellular function(s) between cybrids of varying mtDNA haplogroups can be attributed to their different mtDNA. Previously published data within our laboratory illustrated that transmitochondrial cybrids with mitochondria from either mtDNA haplogroup H (Southern Europe) or J (Northern Europe), exhibited varying levels of cellular metabolism, cell viability, and gene expression levels *in vitro*. J mtDNA haplogroup cybrids showed metabolism levels similar to those of cancer cells, as defined by the *Warburg Phenomenon* (Kenney et al. 2014a; Kenney et al. 2013; Patel et al. 2019).

We designed the present study to observe the effect(s) that mtDNA from L (African maternal descent), [A+B] (Hispanic maternal descent), and D (Asian maternal descent) haplogroups have on cellular function(s) after cisplatin treatment. Our findings demonstrated that treating cybrids containing varying mtDNA haplogroups with cisplatin yielded differing levels of cellular metabolic activity, cytotoxicity, and gene expression. These findings support the hypothesis that mtDNA representing different racial/ethnic groups likely plays a role in the effectiveness and side effects induced by cisplatin.

Materials & Methods

Creation of Cybrid Cells

Cytoplasmic hybrids (cybrids), cell lines with identical nuclear genomes but different mitochondrial genomes, were created and used in the fifth passage for all experiments. All experiments were carried out in accordance with the Institutional Review Board at the University of California, Irvine, (IRB #2003-3131) and were consistent with Federal guidelines. Cybrid cells were created using platelets isolated from peripheral blood that was fused with Rho0 (mtDNA free) ARPE-19 cells (*Fig. 1*) (Patel et al. 2019; Soe et al. April 2011). The mtDNA haplogroups for each subject and cybrid cell line were identified using polymerase chain reaction (PCR) along with restriction enzyme digestion and mtDNA sequencing as described previously in the study conducted by Patel *et al.* on H and J mtDNA haplogroup cybrid cells (Patel et al. 2019).

Sequencing of mtDNA from L, A, B, and D Cybrids

DNA was extracted from the individual cybrids (n = 7 for L cybrids, n = 4 for [A+B] cybrids, and n = 3 for D cybrids) using a kit (DNeasy Blood and Tissue Kit, Qiagen, Germantown, MD). Sequencing techniques similar to those previously described in the study between H and J mtDNA haplogroup cybrids were conducted (Patel et al. 2019). Next Generation Sequencing (NGS) technology was used to sequence both strands of mtDNA independently in both directions. This was done to quantitate the haplogroup-defining single nucleotide polymorphisms (SNPs), private SNPs (not defining haplogroups), and low-frequency heteroplasmy SNPs across the entire mitochondrial genome. NGS technology is capable of deep sequencing (average sequencing depth of 30,000; range 1,000 to 100,000) and accurately differentiates low-frequency mtDNA heteroplasmy SNPs from DNA modification artifacts. The mtDNA sequences were analyzed using HaploGrep (www.haplogrep.uibk.ac.at) to identify the mtDNA haplogroups (*Figs. 2-4, Table 1*). Defined SNP changes between the L, [A+B], and D cybrids were obtained using www.Phylotree.org. and Amino acid changes and any associated pathogenesis resulting from differences in SNP variants were verified using www.MitoMap.com and/or www.hmtvar.uniba.it. The rs numbers were identified using www.ncbi.nlm.nih.gov/snp. All of the SNPs identified had a Quality Score of 100 (A Phred-scaled quality score assigned by the variant caller) and Passed all of the Filters (Patel et al. 2019) (*Table 2)*.

Cybrid Cell Lines Culture

Cybrid cell lines containing mitochondria with either L, [A+B], or D haplogroups were cultured in flasks until confluent. They were then plated on a 96-well or 24-well plates depending on the assay. The MTT, JC1 and LDH experiments were performed on 7 different L cybrids, each with mitochondria from different individuals. The [A+B] cybrids represented 4 different individuals. The D cybrids represented 3 different subjects. Each treatment condition was run in quadruplicate and the experiments repeated twice. The mean values of all cybrids were calculated for both experiments individually. Then these individual means were combined by haplogroup (L versus [A+B] versus D) for the final analyses.

Cells were plated in 96-well plates with each well containing 50,000 cells. After 24 hours, media were removed, and cells were treated with 100 µL of 40 µM concentration of cisplatin (given as a gift from Professor Bota, UCI Medical Director, Neuro-Oncology Program). Generally, the concentration of cisplatin used to treat cancer cells for 48 hours is 10 µM. However, a previous study done by Patel *et. al* on ARPE-19 cybrids containing either H or J mtDNA haplogroups found that the concentration best fit to inhibit these cells was 40 µM. This was concluded via IC-50 analysis which demonstrates the concentration of cisplatin necessary to inhibit cell viability by 50%. As a result, the 40 µM concentration was selected for treatment in the current study (Patel et al. 2019). Plates were then incubated at 37° C for another 48 hours.

Cellular Metabolic Activity Measured by Tetrazolium Dye (MTT) Assay

The MTT assay was conducted to assess cellular metabolic activity, which was in turn correlated to ATP production and overall cell viability. After the 48-hour incubation period, 10 µL of MTT solution (3-(4,5-dimethylthiazol-2-yl)-2,5-diphenyltetrazolium bromide, (Biotium, Hayward, CA) was added to the 100 µL of medium in each well. Plates were then incubated at 37° C for 2 hours. 100 µL of DMSO was directly added into the medium in each well and pipetted up and down until thoroughly mixed. Absorbance was measured on an absorbance reader (BioTek, ELX 808, Winooski, VT) at 570 nm (measured) and 630 nm (reference). The reference absorbance value was subtracted from the measured value in order to attain true absorbance values. All values were normalized to the average metabolic activity of the untreated-L cybrids. Average values for the cybrids were then compared to the respective untreated cybrids using a two-tailed t-test (GraphPad Prism Software, Inc, San Diego, CA). $P \leq 0.05$ was deemed statistically significant. Each treatment condition was run in quadruplicate, and the entire experiment was repeated twice.

Mitochondrial Membrane Potential (ΔΨm) Assay (JC-1 Assay)

L, [A+B], and D cybrids were plated in 24-well plates (100,000 cells/well), incubated 24 hours and, treated with 0 or 40µM of cisplatin for another 48 hours. JC-1 reagent (5,5',6,6'-tetrachloro-1,1',3,3'- tetraethylbenzimidazolylcarbocyanine iodide) (Biotium, Hayward, CA) was added to cultures for 15 minutes. Similar to the study conducted by Patel *et. al*, a Gemini XPS Microplate Reader (Molecular Devices) was used to measure fluorescence for red (excitation 550 nm and emission 600 nm) and green (excitation 485 nm and emission 545 mm) wavelengths. Intact mitochondria with normal ΔΨm fluoresced red, while cells with decreased ΔΨm fluoresced green. Experiments were then analyzed in quadruplicate, and the entire experiment was repeated twice. All values were normalized to the average of the untreated-L cybrids, and cisplatin-treated cybrids were compared to untreated cybrids using a two-tailed t-test to assess for statistical significance (GraphPad Prism Software, Inc.) (Patel et al. 2019).

Mitochondrial Membrane Potential (ΔΨm) Assay (IncuCyte® Live Cell Analyzer With ARPE-19 Cells)

After cisplatin treatment, the cybrids showed decreased metabolic activity but the mitochondrial membrane potentials remained unchanged, which was unexpected. Therefore, we conducted additional experiments using the ARPE-19 cell line evaluated with the IncuCyte® Live Cell Analyzer (Sartorius, City, State) and the Nuclight Rapid Red probe (A549 NucLight Red, cat # 4491) that allowed for comparison of growth/proliferation over 40 hours in cultures treated with 20 µM or 40 µM cisplatin (n = 7 per treatment condition). The IncuCyte® Analyzer captures changes in probes fluorescence and morphologic images in real time. The mitochondrial membrane potential was measured with the JC-1 reagent (5,5',6,6'-tetrachloro-1,1',3,3'-tetraethylbenzimidazolyl-carbocyanine iodide) (Biotium, Hayward, CA) that was added to cultures for 15 minutes. Fluorescence was measured for red (excitation 550 nm and emission 600 nm) and green (excitation 485 nm and emission 545 mm) wavelengths. Intact mitochondria with

normal ΔΨm appeared red, while cells with decreased ΔΨm were in a green fluorescent state (n = 7 wells per treatment condition).

The ARPE-19 cells (ATCC, Manassas, VA); (Invitrogen-Gibco, Carlsbad, CA), which are the wildtype of the Rho*0* receipt cells of the cybrids, were cultured in Dulbecco's modified Eagle's and Ham's nutrient mixture F-12 (1:1 mixture, vol/vol), 0.37% sodium bicarbonate, 0.058% L-glutamine, 10% fetal bovine serum, antibiotics (100U/ml penicillin G, 0.1mg/ml streptomycin sulfate, 10µg/mL gentamicin), 10mM non-essential amino acids, and an anti-fungal agent (amphotericin-B 2.5µg/mL). ARPE-19 cells are a homogeneous, retinal-derived cell line with functional and structural properties similar to human retinal pigment epithelial (RPE) cells (Dunn et al. 1996). All cells within the ARPE-19 culture express RPE-specific markers such as CRALBP, BEST1, and RPE-65 (Moustafa et al. 2017).

Cytotoxicity Assay - Lactate Dehydrogenase Assay (LDH Assay)

L, [A+B], and D cybrids were plated in 96-well plates (10,000 cells/ well) for 24 hours and treated with 0 or 40µM of cisplatin for another 48 hours. 50 µM of supernatant containing the released LDH from each corresponding well was transferred to a new 96-well plate, and 50 µM of reaction mixture was subsequently added and gently mixed. The plates were incubated at room temperature for 30 minutes, and the resulting reactions were stopped by adding 50 µM of stop solution to each well. Absorbance readings were taken at both 490 nm and 680 nm using an absorbance reader (BioTek, ELX 808, Winooski, VT). Percent cytotoxicity levels were calculated using the equation (Treated LDH level – spontaneous LDH level) divided by (Maximum LDH level – spontaneous LDH level) multiplied by one hundred. Average percent cytotoxicity levels were calculated for each ethnic population, normalized to the L haplogroup, and then compared using a two-tailed t-test. $P \leq 0.05$ was deemed statistically significant. Cytotoxicity levels were analyzed, each treatment condition was run in quadruplicate and the entire experiment was repeated three separate times.

RNA Isolation, Quantitative-Real Time PCR (qRT-PCR)

L, [A+B], and D cybrids were plated in six-well plates (500,000 cells/well) and incubated for 24 hours. Cybrid cells were then treated with culture media containing either 0 or 40µM of cisplatin for an additional 48 hours. Trypsinized cells were pelleted, and RNA was isolated according to the manufacturer's protocol (RNeasy Kit, Qiagen, Valencia, CA). Following RNA quantification (Nanodrop 1000, Thermoscientific, Wilmington, DE), the cDNA was synthesized from 2µg of RNA (QuantiTect Reverse Transcription Kit, Qiagen), and used for qRT-PCR (StepOnePlus instrument; Applied Biosystems, Carlsbad, CA). Proprietary, predesigned and validated SYBR Green-based primer assays were used (QuantiTect Primer Assays, Qiagen). Qiagen, the source for the primer assays does not release the sequence of their primers and an internal reference gene number (rs#) is not provided, however, the identity of each primer assay can be identified via the gene's GenBank accession number (NM) (https://geneglobe.qiagen.com/product-

groups/quantitect-primer-assays). Cancer-related nuclear genes were selected as they are typically the target for many chemotherapeutic treatments and presently have medications that target them. They were examined to understand how variations in mtDNA haplogroups affect retrograde signaling (mitochondria to nucleus) in cells that only vary in their mtDNA. The genes analyzed included *ALK* (Anaplastic Lymphoma Receptor Tyrosine Kinase, NM_004304), *BRCA1* (DNA Repair Associated, NM_007294), *EGFR* (Epidermal Growth Factor Receptor 1, NM_005228), and *ERBB2*/*HER2* (Erb-b2 Receptor Tyrosine Kinase 2, NM_004448) genes. Similar to the study done by Patel *et. al*, target cycle thresholds (Ct) values were first compared to the Ct values of reference genes, and then, comparisons between untreated and cisplatin-treated values (ΔΔCt) were evaluated for statistical significance. Fold differences were quantified using the equation $2^{(\Delta\Delta Ct)}$, and the values for each sample were normalized to that of the untreated. This was done separately for each haplogroup in order to identify a starting base expression level and observe the gene expression fold difference after cisplatin treatment (*Tables 3-4*) (Patel et al. 2019).

Statistical Analysis

Statistical analysis of the data were performed by ANOVA (GraphPad Prism, version 5.0). Newman-Keuls multiple-comparison or the two-tailed *t*-tests were used to compare the data within each experiment. Results were normalized to that of the average untreated-L cybrid for each cell study. $P \leq 0.05$ was considered statistically significant. Error bars representing standard deviation (SD) as well as standard error of the mean (SEM) have been graphed for each assay (Patel et al. 2019).

Results

Creation of L, A, B, and D Cybrids

Figure 1 represents the cybrid cell creation process resulting in cells with identical nuclei but differing mtDNA haplogroups. The mtDNA haplogroups for each subject and cybrid cell line were verified using polymerase chain reaction (PCR) along with restriction enzyme digestion and mtDNA sequencing as described previously in the study conducted by Patel *et al.* on H and J mtDNA haplogroup cybrid cells (L cybrids, n = 7; [A+B] cybrids, n = 4; and D cybrids, n = 3) (Patel et al. 2019).

Sequencing of mtDNA from L, A, B, and D Cybrids

The entire mtDNA from the L, A, B, and D cybrids were sequenced using Next Generation Sequencing (NGS) technology. *Table 1* summarizes the mtDNA haplogroup, age and gender for the subjects in this study. *Figures 2-4* show individual mtDNA SNPs that define the haplogroup classification of each cybrid. The private SNPs are those that do not define the L, A, B, or D haplogroups (non-haplogroup defining). The unique SNPs are those SNPs not listed in www.mitomap.org or other programs (*Figs. 2-4, Table 1)* (Patel et al. 2019). Values in the cell and gene expression studies are averages and do not represent any particular SNP variant within

one haplogroup. They are instead representative of the haplogroup-defining SNPs common among all cybrids within a haplogroup. SNP Variants associated with the L, [A+B], and D mtDNA haplogroups as well as the location of the mtDNA nucleotide change, the base pairs changed, their associated rs number, and any associated pathogenesis found in the literature were identified and assessed. Non-synonymous changes present in some but not all haplogroups tested were found at 4824 A>G, rs ND; 5178 C>A, rs28357984; 5442 T>C, rs3020601; 7146 G>A, rs372136420; 8701 G>A, rs2000975; 8794 C>T , rs2298007; 10398 G>A, rs2853826; and 13105 G>A, rs2853501 (www.hmtvar.uniba.it and www.phylotree.org) (*Table 2*).

Relative Cellular Metabolic Activity of Untreated L, A+B, and D Cybrids

The cellular metabolic activity measured with the MTT assay is representative of the cell viability within the cybrid cultures. The untreated cybrids, representing different maternal ethnic populations (African (L), Hispanic [A+B], or Asian (D) mtDNA haplogroups), had statistically similar relative cellular metabolic activities. All values were normalized to the average of the untreated-L cybrids and displayed as the mean ± SEM (*Fig. 5A*). The distribution of each value was also presented in a dot-plot graph representing mean ± SD (*Fig. 5B*). The untreated-L cybrids (102.4% ± 7.0% SEM; SD = 21.0%, n = 7) had similar relative cellular metabolic activity when compared to the untreated-D cybrids (111.7% ± 4.3% SEM; SD = 11.3%, n = 3, p = 0.311) and the untreated-[A+B] cybrids (95.0% ± 8.5% SEM; SD = 20.9%, n = 4, p = 0.512). Untreated-[A+B] cybrids showed similar cellular metabolic activity compared to the untreated-D cybrids (p = 0.0933). Experiments were analyzed in quadruplicate, and the entire experiment was repeated twice.

Relative Cellular Metabolic Activity of L, A+B, and D Cybrids After Cisplatin Treatment

We found significantly reduced cellular metabolic activity after cisplatin treatment in the L, [A+B], and D cybrids compared to their respective untreated controls (*Fig. 6AandB*). All values were normalized to the average of the untreated-L cybrids and displayed as the mean ± SEM (*Fig. 6A)*. The distribution of each value was also presented in a dot-plot graph representing mean ± SD (*Fig. 6B*). The cisplatin-treated-L cybrids showed the greatest reduction in relative cellular metabolic activity compared to the untreated-L cybrids (75.0% ± 6.7% SEM; SD = 20.0%, n = 7; 102.4% ± 7.0% SEM; SD = 21.0%, n = 7, respectively) (p = 0.0117). The cisplatin-treated-D cybrids showed a significant decrease in cell viability compared to the untreated-D cybrids (86.9% ± 1.6% SEM; SD = 4.3%, n = 3; 111.7% ± 4.3% SEM; SD = 11.3%, n = 3, respectively) (p = 0.0001). The cisplatin-treated-[A+B] cybrids also had a statistically significant decrease in cellular metabolic activity compared to their respective untreated-[A+B] cybrids (70.3% ± 4.5% SEM; SD = 11.1%, n = 4; 95.0% ± 8.5% SEM; SD = 20.9%, n = 4, respectively) (p = 0.0285) (*Fig. 6AandB*). Each treatment was run in quadruplicate and the entire experiment was repeated twice.

Mitochondrial Membrane Potential (ΔΨm) After Cisplatin Treatment

Mitochondrial membrane potentials for untreated and treated cybrid cells were measured. All values were normalized to the average of the untreated-L cybrids and displayed as the mean ± SEM (*Fig 7A)*. The distribution of each value was also presented in a dot-plot graph representing mean ± SD (*Fig. 7B*). Results indicated that there was no significant difference in mitochondrial membrane potential in the cisplatin-treated cybrids compared to the untreated cybrids. Cisplatin-treated-L cybrids had a relative mitochondrial membrane potential of 108.4% ± 8.2% SEM; SD = 21.8% versus untreated-L cybrids (101.0% ± 11.2% SEM; SD = 29.5%, n = 7, p = 0.602). Cisplatin-treated-[A+B] displayed 136.5% ± 33.9% SEM; SD = 67.8% versus untreated-[A+B] cybrids (147.5% ± 42.0% SEM; SD = 84.0%, n = 4, p = 0.845). The cisplatin-treated-D cybrids were observed to have a relative mitochondrial membrane potential of 115.0% ± 3.5% SEM, SD = 7.0% versus the untreated-D cybrids (127.3% ± 20.1% SEM; SD = 40.3%, n = 3, p = 0.571) (*Fig. 7AandB*). Each treatment was run in quadruplicate and the entire experiment was repeated twice.

Mitochondrial Membrane Potential (ΔΨm) Assay (IncuCyte® Live Cell Analyzer With ARPE-19 Cells)

After cisplatin treatment, the cybrids showed decreased metabolic activity but the mitochondrial membrane potentials remained unchanged, which was unexpected. Therefore, we conducted additional experiments using the ARPE-19 cell line that allowed for comparison of growth/proliferation over 40 hours in cultures treated with 20 μM or 40 μM cisplatin (n = 7 per treatment condition). All values were displayed as the mean ± SD. Over the first 8 hours of culture, the untreated and cisplatin-treated ARPE-19 cells showed similar rates of growth (*Fig. 8A*). By 10 hours the untreated ARPE-19 cells showed an increasing slope of growth compared to the 20 μM and 40 μM cultures that were stagnant in their growth. By 40 hours, the untreated had a 2-fold higher number of cells than cisplatin-treated cultures. (Untreated 1969 ± 115 standard deviation (SD)), versus 20 μM (1023 ± 81 SD, p = 0.0006) and 40 μM (945 ± 74 SD, p = 0.0001) (At 40 hours, the ΔΨm levels were similar between the untreated AREP-19 (1.8993 ± 0.145 SD) versus 20 μM (2.0698 ± 0.161 SD, p = NS) and 40 μM (2.0520 ± 0.162 SD, p = NS) cisplatin-treated ARPE-19 cultures (*Fig. 8B)*.

Lactate Dehydrogenase Cytotoxicity After Cisplatin Treatment

The cytotoxicity levels of each of the cybrids were measured with the lactate dehydrogenase (LDH) assay. All values were normalized to the average of the untreated-L cybrids and displayed as the mean ± SEM (*Fig. 9A)*. The distribution of each value was also presented in a dot-plot graph representing mean ± SD (*Fig. 9B*). When normalized to the L cybrids, there were significantly higher LDH cytotoxicity levels in L cybrids compared to [A+B] cybrids (111.5% ± 16.5% SEM; SD = 40.5%, n = 7 versus 41.8% ± 9.8% SEM; SD = 16.9%, n = 4, respectively) (p = 0.0270). The D cybrids trended lower LDH levels but they were not significant (48.9% ± 20.2% SEM; SD = 35.0% , n = 3, p = 0.0576) compared to the L cybrids. LDH cytotoxicity

levels between the [A+B] and D cybrids were not statistically different (p = 0.766) (*Fig. 9AandB*). The entire experiment was repeated three separate times.

Gene Expression Levels in L, [A+B], and D Cybrids After Cisplatin Treatment

ALK (Anaplastic Lymphoma Kinase): Transcription levels for L cybrids and the combined [A+B] cybrids dropped significantly after cisplatin treatment (0.18 fold ± 0.097, n = 7, p < 0.0001; 0.17 fold ± 0.095, n = 4, p = 0.0001, respectively), while the D cybrids had no significant change in *ALK* gene expression (n = 3, p = 0.290) (*Tables 3-4*).

BRCA1 (Breast Cancer 1): Gene expression levels for all cybrids (L, [A+B], and D) did not significantly change after treatment with cisplatin compared to untreated-control cybrids (n = 7, 4, 3, p = 0.356, 0.294, p = 0.158, respectively) (*Tables 3-4*).

EGFR (Epidermal Growth Factor Receptor 1): After cisplatin treatment, cybrids containing L and D mtDNA haplogroups had no significant change in *EGFR* gene expression compared to their respective untreated-controls (n = 7, p = 0.301 and n = 3, p = 0.218, respectively). However, cisplatin-treated cybrids containing [A+B] mtDNA haplogroups significant decreased in *EGFR* gene expression levels when compared to untreated-[A+B] cybrids (0.50 fold ± 0.17, n = 4, p = 0.0246) **(***Tables 3-4***)**.

ERBB2/HER2 (Erb-b2 Receptor Tyrosine Kinase 2): Similar to the *BRCA1* gene expression levels, *ERBB2/HER2* gene expression levels were not significantly different after cisplatin treatment in any of the cybrid cell lines (L, [A+B], and D) tested (n = 7, 4, 3; p = 0.839, 0.379, 0.325, respectively) **(***Tables 3-4***)**.

Discussion

Sequencing of the Entire mtDNA

The NGS technology used to analyze the mtDNA from each of the L, A, B, and D cybrids showed that the majority of SNPs identified were haplogroup defining. The private SNPs (non-haplogroup defining), unique SNPs (not listed in www.mitomap.org), and heteroplasmy SNPs were found in individual cybrids and not throughout all of the L, A, B, or D cybrids. Similar to the study comparing cybrids with H and J mtDNA haplogroups, this suggests that the differential retrograde signaling between the L, A, B, and D mtDNA haplogroups is due to the accumulation of the haplogroup defining SNPs rather than a single mutation or private SNP (Patel et al. 2019). These data are also consistent with another cybrid study which used allelic discrimination and Sanger sequencing to identify the mtDNA haplogroups (Atilano et al. 2015). NGS technology was used for deep sequencing of the mtDNA (ranging from 1,000 to 100,000, with an average depth of 30,000), which allowed for low-level heteroplasmy to be reliably identified (Patel et al. 2019). This method helps distinguish artifact from low-level heteroplasmy because both strands

of mtDNA are independently sequenced in both directions. The role of mtDNA haplogroups in retrograde signaling is still under investigation, and many pathways may still be unidentified.

Haplogroup-defining SNPs were analyzed and the nucleotide changes between the L, [A+B], and D cybrids were identified (*Table 2).* Non-synonymous changes (causing a change in amino acid) present in some but not all haplogroups tested were found at eight locations. Related pathogenesis to these SNP variants have been associated with diseases such as asthenospermia, atherosclerosis, breast cancer, cardiomyopathy, esophageal cancer, fertilization failure, Fuch's endothelial corneal dystrophy (FECD), glaucoma, diabetes, hypertension, infertility, irritable bowel syndrome, myocardial infarction, neuropathy, osteoarthritis, osteosarcoma, Parkinson's, mobility impairment, neuromuscular disorders, schizophrenia, somatic lung cancer, and thyroid cancer (www.hmtvar.uniba.it and www.phylotree.org) (*Table 2*). One could speculate that these SNP variants may play a role in the differential susceptibility to cisplatin in L, [A+B], and D cybrids because the cybrids have identical nuclei but vary in their mtDNA. Additional studies are needed to better understand the relationship between mtDNA haplogroups and drug susceptibility-related cellular pathways.

Variations within mtDNA in L, A+B. and D cybrids are associated with a differential decline in relative cellular metabolic activity after treatment with cisplatin.

After 48 hours, the untreated L (African maternal descent), [A+B] (Hispanic maternal descent), and D (Asian mitochondrial descent) cybrids had similar levels of cellular metabolic activities.

However, in response to cisplatin treatment, there was a differential decline in relative cellular metabolic activity (L > D > [A+B] cybrids) compared to their respective untreated cultures with the [A+B] cybrids showing the smallest decrease in metabolic activity. One can speculate that if a person with mtDNA containing a more resistant SNP variant, such as haplogroup [A+B], was treated with identical doses of cisplatin compared to an individual with haplogroup L mitochondria, the first individual might experience signs of resistance to the drug, while the latter would experience a significant drop in cellular metabolic activity in the targeted cells. These data suggest that an individual's mtDNA haplogroup profile may play a role in their response to cisplatin treatment, thereby affecting its efficiency and severity when used in chemotherapy. Understanding how pharmacogenomics play a role in patient treatment, particularly, how the patient's mtDNA SNP profile is associated with variations in drug susceptibility, would allow future treatment programs to focus more on an individual's genetic background in order to achieve more effective results (van Gisbergen et al. 2015). Further studies will be required to better understand the relationship between mtDNA SNP variants and differences in drug susceptibility.

Cisplatin treatment induced apoptosis without significantly disrupting mitochondrial membrane potential.

Data from the JC-1 assay indicated that when treated with cisplatin, mitochondrial membrane potential in all cybrids was maintained. Surprisingly, L, [A+B], and D cybrids did not show any significant change in mitochondrial membrane potential after cisplatin treatment. OXPHOS related ATP production is dependent on mitochondrial membrane potential, and a drastic decrease or increase in membrane potential in the intermembrane space results in less efficient ATP production via ATP synthase. Cisplatin is known to disrupt mitochondrial membrane potential by inducing the synthesis of pro-apoptotic proteins such as Bcl-2 family proteins, Bax and Bak, which form porous defects within the outer membrane of the mitochondria and result in the release of apoptotic factors such as Cytochrome *c* into the cytosol, ultimately resulting in cell death (Pabla et al. 2008). However, a failure of the mitochondrial membrane potential to decrease in the case of cybrids containing L, [A+B], or D mtDNA haplogroups, suggests that a decrease in cell viability leading to apoptosis was induced by a mechanism that did not disrupt the proton gradient within the intermembrane space of the mitochondria. In a previous study, it was observed that somatic mtDNA mutations affect apoptosis without affecting ROS levels or OXPHOS (Trifunovic et al. 2005). Additionally, a study on renal cells demonstrated that neither mitochondrial membrane potential nor OXPHOS related ATP production significantly changed at any time during cisplatin exposure (Cummings & Schnellmann 2002).

The ARPE-19 experiments were conducted to verify the cybrid results obtained from the JC-1 mitochondrial membrane potential assays. The ARPE-19 experiments showed the 20 μM and 40 μM cisplatin prevented cell proliferation, indicating growth inhibition and decreased cell health but did not cause elimination of the cells. Surprisingly the levels for mitochondrial membrane potential ($\Delta\Psi m$) were similar in the untreated and cisplatin-treated cultures. This assay relies on the ratio of red (healthy) and green (dead cells) to indicate change in $\Delta\Psi m$. The red fluorescence is proportional to the potential but diminished in apoptotic or necrotic cells. In ARPE-19 cultures, the cisplatin caused cells to stain more brightly with both red and green intensity, so the final ratio was unchanged (*Fig. 8A*). This suggests that the cisplatin is not lowering the mitochondrial membrane potential, which agrees with Kleih and colleagues who observed that ovarian cancer cells treated with cisplatin also maintained their mitochondrial membrane potential (Cocetta et al. 2019; Kleih et al. 2019). Similarly, English et. al found that cisplatin-treated neuronal cells could maintain and restore their mitochondrial membrane potential through the uptake of cisplatin-resistant mitochondria from astrocytes (English et al. 2020).

An alternative pathway leading to apoptosis as a result of cisplatin treatment may be induced by endoplasmic reticulum (ER) stress. A previous study conducted by Gisbergen *et al.* demonstrated that ER stress-related apoptosis was induced as a result of cisplatin treatment (van Gisbergen et al. 2015). In that study, cisplatin treatment caused ER stress, which activated Caspase-12 cleavage and consequently resulted in apoptosis. Additionally, in a study conducted by Cumming *et al.,* another ER-associated protein leading to apoptosis was identified. Inhibition of Ca^{2+}-independent phospholipase A2 (ER-iPLA2) resulted in an increase of cisplatin-induced apoptosis

in primary rabbit proximal tubular cultures (Cummings et al. 2004). In a previous study conducted on ARPE cybrid cells containing either H or J mtDNA haplogroups, J cybrids showed a significant decline in mitochondrial membrane potential after cisplatin treatment, while H cybrids did not (Patel et al. 2019). A decrease in mitochondrial membrane potential would suggest a decrease in OXPHOS related ATP production and an increase in glycolytic ATP production. As indicated by Stewart et al., ρ^0 cells depleted of mitochondria via Ethidium Bromide (EtBr), rely completely on glycolysis for energy production, indicating that OXPHOS inhibition is inversely related to glycolytic ATP production (Stewart et al. 2011). From the study conducted on H and J cybrids, along with the current study, one can speculate that the unique composition of an individual's mtDNA plays a role in their susceptibility to cisplatin treatment. Additional studies are needed to better understand the relationship between mtDNA variants and drug susceptibility.

Cybrids with dissimilar mtDNA haplogroups vary in LDH cytotoxicity after cisplatin treatment.

Lactate Dehydrogenase cytotoxicity levels measured by the LDH assay illustrated varying results for each of the groups examined. The L cybrids exhibited the highest normalized LDH cytotoxicity levels, which were statistically greater than the [A+B] but not the D cybrids ($p = 0.0270$ and $p = 0.0576$, respectively). Additionally, statistical analysis between the [A+B] cybrids and the D demonstrated that the two groups did not have statistically different LDH cytotoxicity levels ($p = 0.766$) (*Fig. 9AandB*). Cisplatin-induced cytotoxicity is primarily by the mediation of covalent purine adducts within the nuclear (n) DNA that result in disruption of transcription and replication, consequently leading to cell death (Dasari & Tchounwou 2014). One can speculate that nDNA adduct formation leading to extracellular cytotoxicity is less prevalent in cybrids containing [A+B] mtDNA haplogroups compared to cybrids containing L mtDNA haplogroups. In a previous study conducted by Kohno *et al.* on cancer cells, it was determined that the prevalence of guanine base sequences within the mtDNA was a determining factor for the ability of cisplatin to bind effectively and form adducts within the DNA, therefore supporting the idea that cisplatin-induced cytotoxicity depended on the unique profile of the individual's mtDNA (Kohno et al. 2015). Variations in cisplatin-induced cytotoxicity between cybrids with different mtDNA may suggest that mtDNA SNP variants play a key role in the extent to which adducts form. Additional studies are needed to better understand the relationship between mtDNA haplogroups and DNA adduct formation.

Variations within mtDNA are associated with modulation of retrograde signaling, resulting in varying nuclear gene expression levels.

Varied Gene Expression Levels Among Experimented mtDNA Haplogroups:

ALK: We examined the *ALK* gene as it is a common biomarker in patients with non-small-cell lung cancer (NSCLC) and is the primary target of many chemotherapeutic treatments used to treat NSCLC and anaplastic large cell lymphomas (ALCL). (Holla et al. 2017). Cybrids

containing L or [A+B] mtDNA haplogroups had significantly decreased ALK gene expression levels compared to their respective untreated controls, while the cybrids containing D mtDNA haplogroups did not have a significant change compared to their respective controls (*Tables 3-4*). The *ALK* gene codes for a receptor tyrosine kinase in the transmembrane region, and plays an important role in early brain and nervous system development (Hallberg & Palmer 2016; Webb et al. 2009). High ALK gene expression values have been associated with neuroblastoma formation, and the presence of non-small cell lung cancers (NSCLC) (Holla et al. 2017). ALK inhibition has also been a chemotherapeutic target in treatments of these cancers. In the cell culture studies, the D cybrids had higher trending relative cellular metabolic activity than that of cybrids containing L or [A+B] mtDNA haplogroups. Accelerated cellular metabolic activity is a fundamental characteristic of cancer cells, and such behavior exhibited by cybrids containing D mtDNA haplogroups may represent cancer cell-like traits (Mizutani et al. 2009). These data are significant as it suggests that gene expression values in nuclear genes can be altered depending on the particular mtDNA haplogroup present (Cocetta et al. 2019; da Cunha et al. 2015; Patel et al. 2019). Our findings support this because all cybrids contained identical nDNA and media culture conditions but differed in their specific mtDNA haplogroups, therefore, it is unlikely that nDNA contributed to the differences in cisplatin susceptibility. This suggests that the variation in mtDNA can modulate retrograde signaling (mitochondria to nucleus) that results in varied gene expression for the *ALK* gene. The mechanism for this occurrence is not fully understood.

EGFR: The *EGFR* gene as it is a biomarker used to evaluate the efficacy of chemotherapeutic treatments for patients with NSCLC (Wang et al. 2018). After cisplatin treatment, cybrid cells containing L and D mtDNA haplogroups had no significant change in *EGFR* gene expression compared to untreated cybrids. However, cybrids containing the [A+B] mtDNA haplogroups had a significant change in *EGFR* gene expression levels and dropped 50.8% ± 17.1% when compared to their respective untreated cybrids ($p = 0.0246$) (*Tables 3-4*). The *EGFR* gene codes for a transmembrane glycoprotein that binds to epidermal growth factors, and expression of this gene is associated with cell proliferation. In an *in vivo* study on patients with NSCLC, degradation of the *EGFR* gene occurred as a result of platinum-based chemotherapy treatment (Wang et al. 2018). Additionally, Wang et al. concluded that the *EGFR* gene became highly unstable as a result of the chemotherapy treatment, and that *EGFR* expression levels dropped significantly in some patients while remaining similar in others (Wang et al. 2018). In a different study conducted *in vivo*, cisplatin treatment resulted in *EGFR* phosphorylation and subsequent ubiquitination and degradation (Ahsan et al. 2010). This indicated that those individuals with decreased *EGFR* levels were more susceptible to negative mutations and, as a result, more susceptible to the treatment than those with no significant decrease in *EGFR* levels. Results from the current study suggest that patients with [A+B] mtDNA haplogroups may express certain factors that result in their *EGFR* gene to become significantly more unstable than patients with L or D mtDNA haplogroups after treatment with cisplatin. These data suggest that expression levels of nuclear genes can be altered depending on the particular mtDNA haplogroup present

(Cocetta et al. 2019; da Cunha et al. 2015; Patel et al. 2019). Our findings show that different mtDNA variants can alter the expression levels the *EGFR* gene.

Similar Gene Expression Levels Among Experimented mtDNA Haplogroups:

BRCA1: The *BRCA1* gene was analyzed because it is a common biomarker used to understand the efficacy of chemotherapeutic treatments in patients with breast and ovarian cancers (Quinn et al. 2007; Welcsh & King 2001). Gene expression levels for all cybrids (L, [A+B], and D) tested did not significantly change, relative to their respective untreated group, after treatment with cisplatin ($p = 0.356$, 0.294, and 0.158 respectively) **(***Tables 3-4***)**. The *BRCA1* gene encodes a nuclear phosphoprotein that plays a role in maintaining genomic stability, and germline mutations within this gene have been highly associated with breast and ovarian cancers (Welcsh & King 2001). In an *in vivo* study conducted by Quinn *et al.*, *BRCA1* gene expression levels were found to be directly correlated with overall survival in patients with ovarian cancer (Quinn et al. 2007). Results from the current study indicate that the variation in mtDNA within the varying cybrids did not significantly change the *BRCA1* levels of the cybrids. This suggests that the L, [A+B], and D mtDNA haplogroups in ARPE cybrids may not have a significant effect on the gene expression pathways associated with the *BRCA1* gene.

ERBB2/HER2: We examined the *ERRB2/HER2* gene as it is a common biomarker used to assess patients with breast cancer (Birnbaum et al. 2009). Similar to the *BRCA1* gene expression levels, *ERBB2/HER2* gene expression levels were not significantly different after cisplatin treatment in all of the cybrid cells (L, [A+B], and D) ($p = 0.839$, 0.379, 0.325 respectively) (*Tables 3-4*). Unlike the *BRCA1* gene, activation and overexpression rather than mutations of this gene have been shown in numerous cancers (breast cancer and ovarian cancer) (Birnbaum et al. 2009). Stable gene expression levels of the *ERBB2/HER2* gene in the L, [A+B], and D cybrids after treatment suggest that the mtDNA SNP variants do not significantly alter pathways associated with *ERBB2/HER2* gene expression.

Conclusions

The efficacy of drug use to treat cancer pathology is determined by the drug's ability to efficiently reduce the effect of or inhibit the disease; however, drug susceptibility has been observed to vary between patients. This variation has been assumed to be a consequence of differences in nDNA, epigenetics, or some other external factors. This study was conducted to assess the consequences of variations within the mtDNA in patients of African, Hispanic, and Asian maternal descent after treatment with the platinum drug cisplatin. The goal of this study was to obtain greater insight into the role of mitochondria, along with its unique genomic information, in drug susceptibility, specifically pathways that promote cisplatin resistance. We used the cybrid model, which are cell lines that contain identical nDNA and media culture conditions but vary only in the specific mtDNA haplogroup profile of each individual. Although nDNA and epigenetic factors may play a role in a patient's response to cisplatin, they would not

account for variations in response to cisplatin in the cybrid model as the only variable is the mitochondrial genome. In summary, cybrid cells with mtDNA haplogroups representing different racial/ethnic populations, displayed unique overall results in the various cell assays and gene expression studies (*Table 3)*. If mtDNA played no role in drug susceptibility, the effects of cisplatin would be expected to be similar throughout the study. However, L, [A+B], and D cybrids displayed dissimilar results, indicating that the variations in mtDNA are associated with variations in drug responses. The mechanism for this variation is not yet fully understood, and further studies are needed to understand this process completely.

Future studies will focus on examining similar biological pathways in cybrid cells lines with other mtDNA haplogroups to obtain a greater understanding of drug susceptibility in relation to maternal ethnic descent. Understanding the role of mtDNA haplogroups in drug resistance could potentially improve drug treatment efficiency *in vivo*, and lead to a greater knowledge of pharmacogenomics as well as lead to a more individualized approach to treatment methods.

Acknowledgements

We wish to thank the subjects who participated in this study. This work was supported by the Discovery Eye Foundation, Polly and Michael Smith, Edith and Roy Carver, and NEI R01 EY0127363 (MCK). Supported by an Unrestricted Departmental Grant from Research to Prevent Blindness. We acknowledge the support of the Institute for Clinical and Translational Science (ICTS) at University of California Irvine. There was no additional external funding received for this study.

References

Ahsan A, Hiniker SM, Ramanand SG, Nyati S, Hegde A, Helman A, Menawat R, Bhojani MS, Lawrence TS, and Nyati MK. 2010. Role of epidermal growth factor receptor degradation in cisplatin-induced cytotoxicity in head and neck cancer. *Cancer research* 70:2862-2869. 10.1158/0008-5472.CAN-09-4294

Amable L. 2016. Cisplatin resistance and opportunities for precision medicine. *Pharmacol Res* 106:27-36. 10.1016/j.phrs.2016.01.001

Atilano SR, Malik D, Chwa M, Cáceres-Del-Carpio J, Nesburn AB, Boyer DS, Kuppermann BD, Jazwinski SM, Miceli MV, Wallace DC, Udar N, and Kenney MC. 2015. Mitochondrial DNA variants can mediate methylation status of inflammation, angiogenesis and signaling genes. *Hum Mol Genet* 24:4491-4503. 10.1093/hmg/ddv173

Birnbaum D, Sircoulomb F, and Imbert J. 2009. A reason why the ERBB2 gene is amplified and not mutated in breast cancer. *Cancer cell international* 9:5-5. 10.1186/1475-2867-9-5

Boulikas T, and Vougiouka M. 2004. Recent clinical trials using cisplatin, carboplatin and their combination chemotherapy drugs (review). *Oncology reports* 11:559-595.

Cocetta V, Ragazzi E, and Montopoli M. 2019. Mitochondrial Involvement in Cisplatin Resistance. *Int J Mol Sci* 20. 10.3390/ijms20143384

678 Cummings BS, McHowat J, and Schnellmann RG. 2004. Role of an endoplasmic reticulum Ca2+-
679 independent phospholipase A2 in cisplatin-induced renal cell apoptosis. *The Journal of*
680 *pharmacology and experimental therapeutics* 308:921-928. 10.1124/jpet.103.060541
681 Cummings BS, and Schnellmann RG. 2002. Cisplatin-induced renal cell apoptosis: caspase 3-
682 dependent and -independent pathways. *J Pharmacol Exp Ther* 302:8-17.
683 10.1124/jpet.302.1.8
684 Czarnecka AM, and Bartnik E. 2011. The Role of the Mitochondrial Genome in Ageing and
685 Carcinogenesis. *Journal of Aging Research* 2011:1-10. 10.4061/2011/136435
686 da Cunha FM, Torelli NQ, and Kowaltowski AJ. 2015. Mitochondrial Retrograde Signaling:
687 Triggers, Pathways, and Outcomes. *Oxid Med Cell Longev* 2015:482582.
688 10.1155/2015/482582
689 Damia G, and Broggini M. 2019. Platinum Resistance in Ovarian Cancer: Role of DNA Repair.
690 *Cancers (Basel)* 11. 10.3390/cancers11010119
691 Dasari S, and Tchounwou PB. 2014. Cisplatin in cancer therapy: molecular mechanisms of
692 action. *European journal of pharmacology* 740:364-378. 10.1016/j.ejphar.2014.07.025
693 Devarajan P, Savoca M, Castaneda MP, Park MS, Esteban-Cruciani N, Kalinec G, and Kalinec F.
694 2002. Cisplatin-induced apoptosis in auditory cells: role of death receptor and
695 mitochondrial pathways. *Hear Res* 174:45-54. 10.1016/s0378-5955(02)00634-2
696 Dunn KC, Aotaki-Keen AE, Putkey FR, and Hjelmeland LM. 1996. ARPE-19, a human retinal
697 pigment epithelial cell line with differentiated properties. *Exp Eye Res* 62:155-169.
698 10.1006/exer.1996.0020
699 English K, Shepherd A, Uzor NE, Trinh R, Kavelaars A, and Heijnen CJ. 2020. Astrocytes rescue
700 neuronal health after cisplatin treatment through mitochondrial transfer. *Acta*
701 *Neuropathol Commun* 8:36. 10.1186/s40478-020-00897-7
702 Florea A-M, and Büsselberg D. 2011. Cisplatin as an Anti-Tumor Drug: Cellular Mechanisms of
703 Activity, Drug Resistance and Induced Side Effects. *Cancers* 3:1351-1371.
704 10.3390/cancers3011351
705 Gottesman MM, Lavi O, Hall MD, and Gillet JP. 2016. Toward a Better Understanding of the
706 Complexity of Cancer Drug Resistance. *Annu Rev Pharmacol Toxicol* 56:85-102.
707 10.1146/annurev-pharmtox-010715-103111
708 Ha Y-N, Sung HY, Yang S-D, Chae YJ, Ju W, and Ahn J-H. 2018. Epigenetic modification of α-N-
709 acetylgalactosaminidase enhances cisplatin resistance in ovarian cancer. *The Korean*
710 *journal of physiology & pharmacology : official journal of the Korean Physiological*
711 *Society and the Korean Society of Pharmacology* 22:43-51. 10.4196/kjpp.2018.22.1.43
712 Hallberg B, and Palmer RH. 2016. The role of the ALK receptor in cancer biology. *Annals of*
713 *Oncology* 27:iii4-iii15. 10.1093/annonc/mdw301
714 Han XJ, Shi SL, Wei YF, Jiang LP, Guo MY, Wu HL, and Wan YY. 2017. Involvement of
715 mitochondrial dynamics in the antineoplastic activity of cisplatin in murine leukemia
716 L1210 cells. *Oncol Rep* 38:985-992. 10.3892/or.2017.5765
717 Holla VR, Elamin YY, Bailey AM, Johnson AM, Litzenburger BC, Khotskaya YB, Sanchez NS, Zeng
718 J, Shufean MA, Shaw KR, Mendelsohn J, Mills GB, Meric-Bernstam F, and Simon GR.
719 2017. ALK: a tyrosine kinase target for cancer therapy. *Cold Spring Harbor molecular*
720 *case studies* 3:a001115-a001115. 10.1101/mcs.a001115

721 Housman G, Byler S, Heerboth S, Lapinska K, Longacre M, Snyder N, and Sarkar S. 2014. Drug
722 Resistance in Cancer: An Overview. *Cancers* 6:1769-1792. 10.3390/cancers6031769
723 Jarrett S, Lin H, Godley B, and Boulton M. 2008. Mitochondrial DNA damage and its potential
724 role in retinal degeneration. *Progress in Retinal and Eye Research* 27:596-607.
725 10.1016/j.preteyeres.2008.09.001
726 Jing L, Su L, and Ring BZ. 2014. Ethnic background and genetic variation in the evaluation of
727 cancer risk: a systematic review. *PLoS ONE* 9:e97522. 10.1371/journal.pone.0097522
728 Kenney MC, Chwa M, Atilano SR, Falatoonzadeh P, Ramirez C, Malik D, Tarek M, Cáceres-del-
729 Carpio J, Nesburn AB, Boyer DS, Kuppermann BD, Vawter M, Jazwinski SM, Miceli M,
730 Wallace DC, and Udar N. 2014a. Inherited mitochondrial DNA variants can affect
731 complement, inflammation and apoptosis pathways: insights into mitochondrial-nuclear
732 interactions. *Hum Mol Genet* 23:3537-3551. 10.1093/hmg/ddu065
733 Kenney MC, Chwa M, Atilano SR, Falatoonzadeh P, Ramirez C, Malik D, Tarek M, del Carpio JC,
734 Nesburn AB, Boyer DS, Kuppermann BD, Vawter MP, Jazwinski SM, Miceli MV, Wallace
735 DC, and Udar N. 2014b. Molecular and bioenergetic differences between cells with
736 African versus European inherited mitochondrial DNA haplogroups: Implications for
737 population susceptibility to diseases. *Biochimica et Biophysica Acta (BBA) - Molecular*
738 *Basis of Disease* 1842:208-219. 10.1016/j.bbadis.2013.10.016
739 Kenney MC, Chwa M, Atilano SR, Pavlis JM, Falatoonzadeh P, Ramirez C, Malik D, Hsu T, Woo G,
740 Soe K, Nesburn AB, Boyer DS, Kuppermann BD, Jazwinski SM, Miceli MV, Wallace DC,
741 and Udar N. 2013. Mitochondrial DNA Variants Mediate Energy Production and
742 Expression Levels for CFH, C3 and EFEMP1 Genes: Implications for Age-Related Macular
743 Degeneration. *PLoS ONE* 8:e54339-e54339. 10.1371/journal.pone.0054339
744 Kleih M, Böpple K, Dong M, Gaißler A, Heine S, Olayioye MA, Aulitzky WE, and Essmann F. 2019.
745 Direct impact of cisplatin on mitochondria induces ROS production that dictates cell fate
746 of ovarian cancer cells. *Cell Death Dis* 10:851. 10.1038/s41419-019-2081-4
747 Kohno K, Wang K-Y, Takahashi M, Kurita T, Yoshida Y, Hirakawa M, Harada Y, Kuma A, Izumi H,
748 and Matsumoto S. 2015. Mitochondrial Transcription Factor A and Mitochondrial
749 Genome as Molecular Targets for Cisplatin-Based Cancer Chemotherapy. *International*
750 *journal of molecular sciences* 16:19836-19850. 10.3390/ijms160819836
751 Marrache S, Pathak RK, and Dhar S. 2014. Detouring of cisplatin to access mitochondrial
752 genome for overcoming resistance. *Proc Natl Acad Sci U S A* 111:10444-10449.
753 10.1073/pnas.1405244111
754 Marullo R, Werner E, Degtyareva N, Moore B, Altavilla G, Ramalingam SS, and Doetsch PW.
755 2013. Cisplatin induces a mitochondrial-ROS response that contributes to cytotoxicity
756 depending on mitochondrial redox status and bioenergetic functions. *PLoS ONE*
757 8:e81162. 10.1371/journal.pone.0081162
758 Meijera C, van Luyn MJ, Nienhuis EF, Blom N, Mulder NH, and de Vries EG. 2001. Ultrastructural
759 morphology and localisation of cisplatin-induced platinum-DNA adducts in a cisplatin-
760 sensitive and -resistant human small cell lung cancer cell line using electron microscopy.
761 *Biochemical pharmacology* 61:573-578.
762 Mizutani S, Miyato Y, Shidara Y, Asoh S, Tokunaga A, Tajiri T, and Ohta S. 2009. Mutations in the
763 mitochondrial genome confer resistance of cancer cells to anticancer drugs. *Cancer*
764 *Science* 100:1680-1687. 10.1111/j.1349-7006.2009.01238.x

765 Moustafa MT, Ramirez C, Schneider K, Atilano SR, Limb GA, Kuppermann BD, and Kenney MC.
766 2017. Protective Effects of Memantine on Hydroquinone-Treated Human Retinal
767 Pigment Epithelium Cells and Human Retinal Müller Cells. *J Ocul Pharmacol Ther* 33:610-
768 619. 10.1089/jop.2016.0129
769 O'Byrne KJ, Barr MP, and Gray SG. 2011. The role of epigenetics in resistance to Cisplatin
770 chemotherapy in lung cancer. *Cancers* 3:1426-1453. 10.3390/cancers3011426
771 O'Donnell PH, and Dolan ME. 2009. Cancer Pharmacoethnicity: Ethnic Differences in
772 Susceptibility to the Effects of Chemotherapy. *Clinical Cancer Research* 15:4806-4814.
773 10.1158/1078-0432.CCR-09-0344
774 Pabla N, Huang S, Mi QS, Daniel R, and Dong Z. 2008. ATR-Chk2 signaling in p53 activation and
775 DNA damage response during cisplatin-induced apoptosis. *J Biol Chem* 283:6572-6583.
776 10.1074/jbc.M707568200
777 Park MS, De Leon M, and Devarajan P. 2002. Cisplatin induces apoptosis in LLC-PK1 cells via
778 activation of mitochondrial pathways. *J Am Soc Nephrol* 13:858-865.
779 Patel TH, Norman L, Chang S, Abedi S, Liu C, Chwa M, Atilano SR, Thaker K, Lu S, Jazwinski SM,
780 Miceli MV, Udar N, Bota D, and Kenney MC. 2019. European mtDNA Variants Are
781 Associated With Differential Responses to Cisplatin, an Anticancer Drug: Implications for
782 Drug Resistance and Side Effects. *Frontiers in Oncology* 9:640-640.
783 10.3389/fonc.2019.00640
784 Penta JS, Johnson FM, Wachsman JT, and Copeland WC. 2001. Mitochondrial DNA in human
785 malignancy. *Mutat Res* 488:119-133. 10.1016/s1383-5742(01)00053-9
786 Quinn JE, James CR, Stewart GE, Mulligan JM, White P, Chang GKF, Mullan PB, Johnston PG,
787 Wilson RH, and Harkin DP. 2007. BRCA1 mRNA Expression Levels Predict for Overall
788 Survival in Ovarian Cancer after Chemotherapy. *Clinical Cancer Research* 13:7413-7420.
789 10.1158/1078-0432.CCR-07-1083
790 Rose MC, Kostyanovskaya E, and Huang RS. 2014. Pharmacogenomics of cisplatin sensitivity in
791 non-small cell lung cancer. *Genomics, proteomics & bioinformatics* 12:198-209.
792 10.1016/j.gpb.2014.10.003
793 Siddik ZH. 2003. Cisplatin: mode of cytotoxic action and molecular basis of resistance.
794 *Oncogene* 22:7265-7279. 10.1038/sj.onc.1206933
795 Singh KK, Russell J, Sigala B, Zhang Y, Williams J, and Keshav KF. 1999. Mitochondrial DNA
796 determines the cellular response to cancer therapeutic agents. *Oncogene* 18:6641-6646.
797 10.1038/sj.onc.1203056
798 Soe K, Chwa M, Pham K, Udar N, Jazwinski SM, Miceli M, and Kenney MC. April 2011.
799 Developing Human ARPE-19 Cybrid Cell Lines from Different Haplogroups Related to
800 Age-related Macular Degeneration (AMD). Investigate Ophthalmology & Visual Science.
801 Stewart DJ. 2007. Mechanisms of resistance to cisplatin and carboplatin. *Critical Reviews in*
802 *Oncology/Hematology* 63:12-31. 10.1016/J.CRITREVONC.2007.02.001
803 Stewart JD, Schoeler S, Sitarz KS, Horvath R, Hallmann K, Pyle A, Yu-Wai-Man P, Taylor RW,
804 Samuels DC, Kunz WS, and Chinnery PF. 2011. POLG mutations cause decreased
805 mitochondrial DNA repopulation rates following induced depletion in human fibroblasts.
806 *Biochimica et Biophysica Acta (BBA) - Molecular Basis of Disease* 1812:321-325.
807 10.1016/J.BBADIS.2010.11.012

Tan DS, Mok TS, and Rebbeck TR. 2016. Cancer Genomics: Diversity and Disparity Across Ethnicity and Geography. *J Clin Oncol* 34:91-101. 10.1200/JCO.2015.62.0096

Trifunovic A, Hansson A, Wredenberg A, Rovio AT, Dufour E, Khvorostov I, Spelbrink JN, Wibom R, Jacobs HT, and Larsson NG. 2005. Somatic mtDNA mutations cause aging phenotypes without affecting reactive oxygen species production. *Proc Natl Acad Sci U S A* 102:17993-17998. 10.1073/pnas.0508886102

Tsuyoshi H, Wong VKW, Han Y, Orisaka M, Yoshida Y, and Tsang BK. 2017. Saikosaponin-d, a calcium mobilizing agent, sensitizes chemoresistant ovarian cancer cells to cisplatin-induced apoptosis by facilitating mitochondrial fission and G2/M arrest. *Oncotarget* 8:99825-99840. 10.18632/oncotarget.21076

van Gisbergen MW, Voets AM, Starmans MHW, de Coo IFM, Yadak R, Hoffmann RF, Boutros PC, Smeets HJM, Dubois L, and Lambin P. 2015. How do changes in the mtDNA and mitochondrial dysfunction influence cancer and cancer therapy? Challenges, opportunities and models. *Mutation Research/Reviews in Mutation Research* 764:16-30. 10.1016/j.mrrev.2015.01.001

Wang Y, Ma X, Wei Y, Ma D, and Gong P. 2018. Effect of platinum-based chemotherapy on EGFR gene mutation status in lung adenocarcinoma. *Medicine* 97:e9602-e9602. 10.1097/MD.0000000000009602

Webb TR, Slavish J, George RE, Look AT, Xue L, Jiang Q, Cui X, Rentrop WB, and Morris SW. 2009. Anaplastic lymphoma kinase: role in cancer pathogenesis and small-molecule inhibitor development for therapy. *Expert review of anticancer therapy* 9:331-356. 10.1586/14737140.9.3.331

Welcsh PL, and King M-C. 2001. BRCA1 and BRCA2 and the genetics of breast and ovarian cancer. *Human Molecular Genetics* 10:705-713. 10.1093/hmg/10.7.705

Yáñez JA, Teng XW, Roupe KA, Fariss MW, and Davies NM. 2003. Chemotherapy induced gastrointestinal toxicity in rats: involvement of mitochondrial DNA, gastrointestinal permeability and cyclooxygenase -2. *J Pharm Pharm Sci* 6:308-314.

Yasuda SU, Zhang L, and Huang SM. 2008. The Role of Ethnicity in Variability in Response to Drugs: Focus on Clinical Pharmacology Studies. *Clinical Pharmacology & Therapeutics* 84:417-423. 10.1038/clpt.2008.141

Ziliak D, Gamazon ER, LaCroix B, Kyung Im H, Wen Y, and Huang RS. 2012. Genetic Variation That Predicts Platinum Sensitivity Reveals the Role of miR-193b* in Chemotherapeutic Susceptibility. *Molecular Cancer Therapeutics* 11:2054-2061. 10.1158/1535-7163.MCT-12-0221

Figure 1

Creation of cybrid cells with identical nuclei but varying mtDNA.

Cytoplasmic hybrids (cybrids) were created by fusing ARPE-19 Rho0 (mtDNA free)cells with platelets isolated from peripheral blood from individuals of either L (African), [A+B] (Hispanic), or D (Asian) maternal descent. Rho0cells were initially obtained by treating ARPE-19 cells with small doses of Ethidium Bromide (EtBr) over many passages until they lacked mitochondria. Once the cells were depleted of their mitochondria, they were fused with the obtained platelets using polyethylene glycol fusion. These platelets lacked nuclear (n) DNA, and only contained mitochondrial (mt) DNA. Once fused, the created cybrids contained identical nDNA and the particular mtDNA obtained from the specified patient's platelets. The mtDNA haplogroups for each subject and cybrid cell line were identified using polymerase chain reaction (PCR) along with restriction enzyme digestion and mtDNA sequencing.

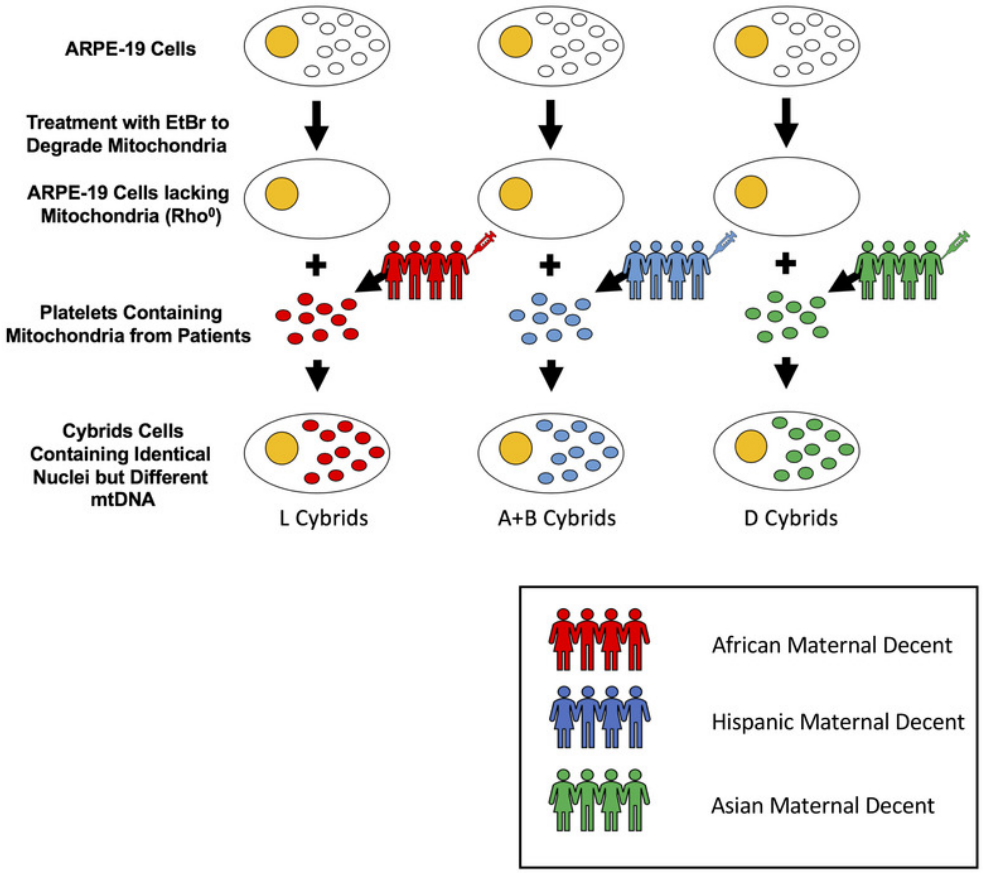
ARPE-19 Cells
Treatment with EtBr to Degrade Mitochondria
ARPE-19 Cells lacking Mitochondria (Rho0)
Platelets Containing Mitochondria from Patients
Cybrids Cells Containing Identical Nuclei but Different mtDNA
L Cybrids
A+B Cybrids
D Cybrids
African Maternal Decent
Hispanic Maternal Decent
Asian Maternal Decent

Figure 2

Mitochondrial SNP variants associated with the various L mtDNA haplogroup subtypes used in this study.

Platelets obtained from patients were sequenced using a kit (DNeasy Blood and Tissue Kit, Qiagen, Germantown, MD), and found to be in the L mtDNA haplogroup (n = 7). The L mtDNA haplogroup is associated with individuals from African maternal descent. The specific variants of those in the L mtDNA haplogroup were identified and their phylogenic tree is displayed. These variants include L0a1a1, L1b1a, L1b1a7, L1b2a, L1c2a1, L2b2, and L3e1a1a. Next Generation Sequencing (NGS) technology was used to sequence both strands of mtDNA independently in both directions. This was done to quantitate the haplogroup-defining single nucleotide polymorphisms (SNPs), private SNPs (not defining haplogroups), and low-frequency heteroplasmy SNPs across the entire mitochondrial genome. The mtDNA sequences were analyzed using HaploGrep (www.haplogrep.uibk.ac.at) to identify the mtDNA haplogroups. SNP variants were verified using www.MitoMap.com, www.Phylotree.org, and/or www.hmtvar.uniba.it.

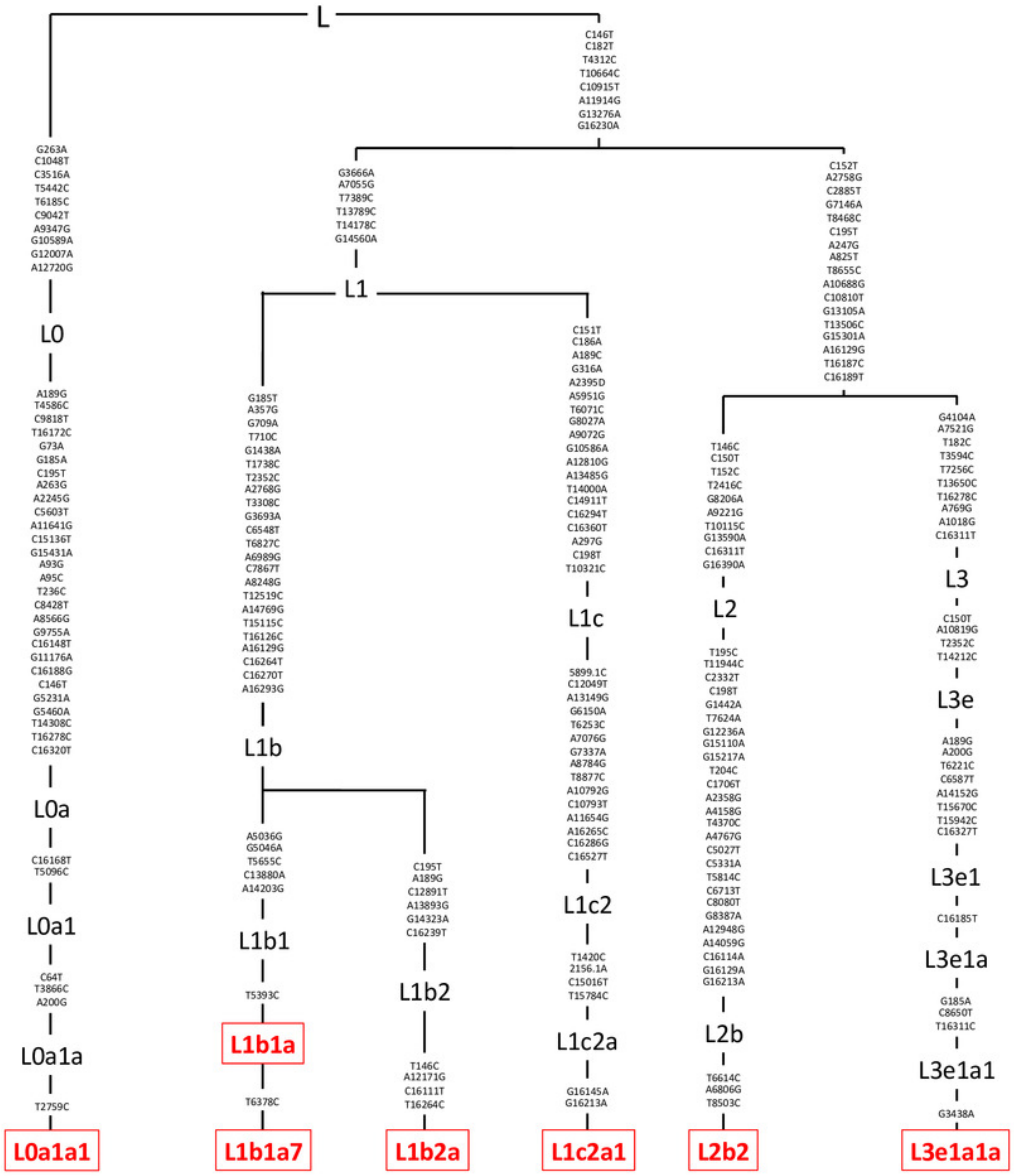
L
C146T C182T T4312C T10664C C10915T A11914G G13276A G16230A
G263A C1048T C3516A T5442C T6185C C9042T A9347G G10589A G12007A A12720G
G3666A A7055G T7389C T13789C T14178C G14560A
C152T A2758G C2885T G7146A T8468C C195T A247G A825T T8655C A10688G C10810T G13105A T13506C G15301A A16129G T16187C C16189T
L0
L1
A189G T4586C C9818T T16172C G73A G185A C195T A263G A2245G C5603T A11641G C15136T G15431A A93G A95C T236C C8428T A8566G G9755A C16148T G11176A C16188G C146T G5231A G5460A T14308C T16278C C16320T
G185T A357G G709A T710C G1438A T1738C T2352C A2768G T3308C G3693A C6548T T6827C A6989G C7867T A8248G T12519C A14769G T15115C T16126C A16129G C16264T C16270T A16293G
C151T C186A A189C G316A A2395D A5951G T6071C G8027A A9072G G10586A A12810G A13485G T14000A C14911T C16294T C16360T A297G C198T T10321C
T146C C150T T152C T2416C G8206A A9221G T10115C G13590A C16311T G16390A
G4104A A7521G T182C T3594C T7256C T13650C T16278C A769G A1018G C16311T
L0a
L1b
L1c
L2
L3
A5036G G5046A T5655C C13880A A14203G
C195T A189G C12891T A13893G G14323A C16239T
5899.1C C12049T A13149G G6150A T6253C A7076G G7337A A8784G T8877C A10792G C10793T A11654G A16265C C16286G C16527T
T195C T11944C C2332T C198T G1442A T7624A G12236A G15110A G15217A T204C C1706T A2358G A4158G T4370C A4767G C5027T C5331A T5814C C6713T C8080T G8387A A12948G A14059G C16114A G16129A G16213A
C150T A10819G T2352C T14212C
C16168T T5096C
L0a1
L1b1
L1b2
L1c2
L2b
L3e
A189G A200G T6221C C6587T A14152G T15670C T15942C C16327T
C64T T3866C A200G
T5393C
T1420C 2156.1A C15016T T15784C
T6614C A6806G T8503C
C16185T
L0a1a
L1b1a
L1b2a
L1c2a
L3e1
G185A C8650T T16311C
T2759C
T6378C
T146C A12171G C16111T T16264C
G16145A G16213A
G3438A
L0a1a1
L1b1a7
L1b2a
L1c2a1
L2b2
L3e1a
L3e1a1
L3e1a1a

Figure 3

Mitochondrial SNP variants associated with the A and B mtDNA haplogroups used in this study.

Platelets obtained from patients were sequenced using a kit (DNeasy Blood and Tissue Kit, Qiagen, Germantown, MD), and found to be in the A or B mtDNA haplogroups (n = 4). (A) The A mtDNA haplogroup is associated with individuals from Hispanic maternal descent. The specific variants of those in the A mtDNA haplogroup were identified and their phylogenic tree is displayed. These variants include A2 and A2w. (B) The B mtDNA haplogroup is also associated with individuals from Hispanic maternal descent. The specific variants of those in the B mtDNA haplogroup were identified and their phylogenic tree is displayed. These variants include B and B2a. Next Generation Sequencing (NGS) technology was used to sequence both strands of mtDNA independently in both directions. This was done to quantitate the haplogroup-defining single nucleotide polymorphisms (SNPs), private SNPs (not defining haplogroups), and low-frequency heteroplasmy SNPs across the entire mitochondrial genome. The mtDNA sequences were analyzed using HaploGrep (www.haplogrep.uibk.ac.at) to identify the mtDNA haplogroups. SNP variants were verified using www.MitoMap.com, www.Phylotree.org, and/or www.hmtvar.uniba.it.

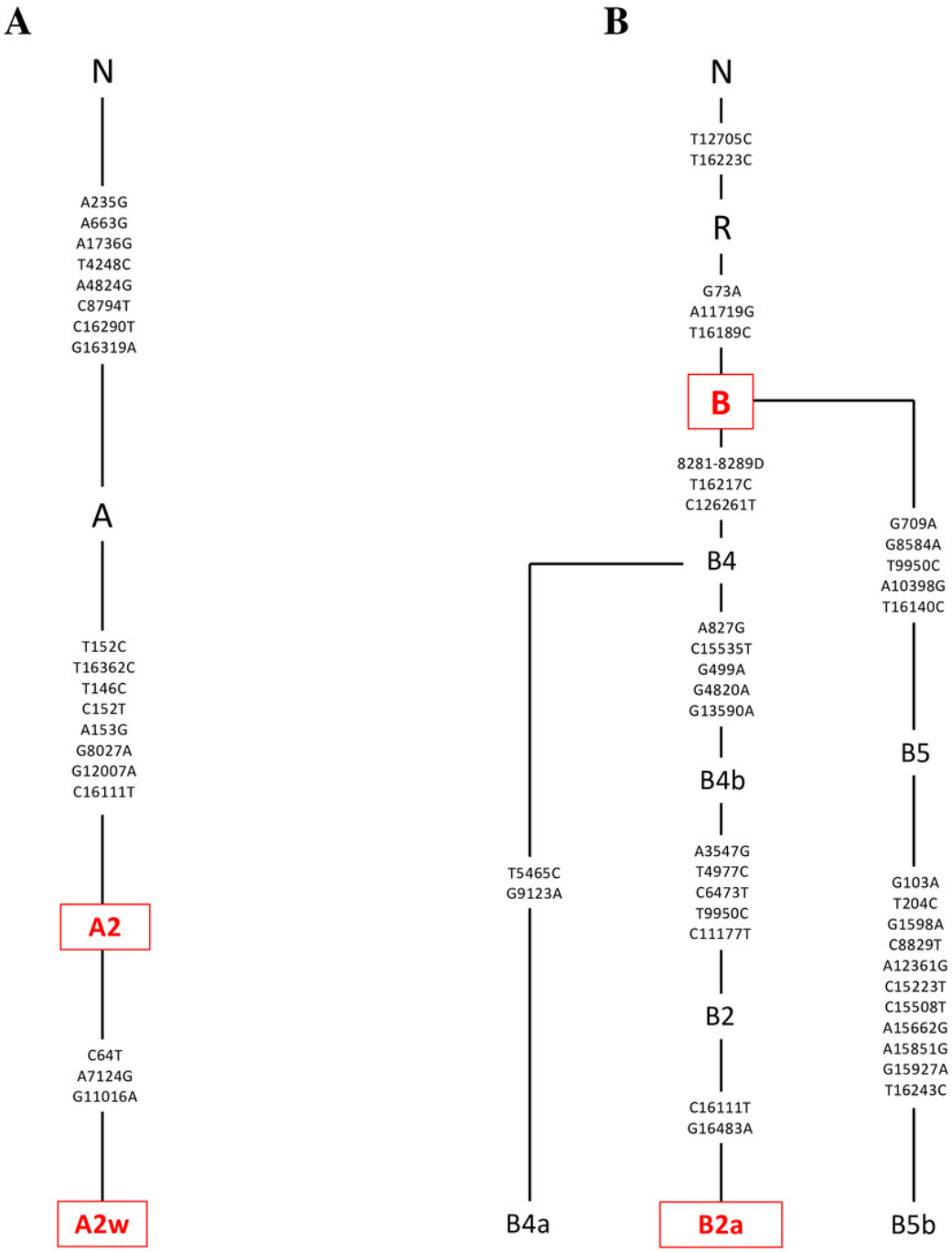
A
N
A235G
A663G
A1736G
T4248C
A4824G
C8794T
C16290T
G16319A
A
T152C
T16362C
T146C
C152T
A153G
G8027A
G12007A
C16111T
A2
C64T
A7124G
G11016A
A2w
B
N
T12705C
T16223C
R
G73A
A11719G
T16189C
B
8281-8289D
T16217C
C126261T
B4
T5465C
G9123A
B4a
A827G
C15535T
G499A
G4820A
G13590A
B4b
A3547G
T4977C
C6473T
T9950C
C11177T
B2
C16111T
G16483A
B2a
G709A
G8584A
T9950C
A10398G
T16140C
B5
G103A
T204C
G1598A
C8829T
A12361G
C15223T
C15508T
A15662G
A15851G
G15927A
T16243C
B5b

Figure 4

Mitochondrial SNP variants associated with the specific D mtDNA haplogroup types used in this study.

Platelets obtained from patients were sequenced using a kit (DNeasy Blood and Tissue Kit, Qiagen, Germantown, MD), and found to be in the D mtDNA haplogroup (n = 3). The D mtDNA haplogroup is associated with individuals from Asian maternal descent. The specific variants of those in the D mtDNA haplogroup were identified and their phylogenic tree is displayed. These variants include D4a2b, D4a6, and D4d. Next Generation Sequencing (NGS) technology was used to sequence both strands of mtDNA independently in both directions. This was done to quantitate the haplogroup-defining single nucleotide polymorphisms (SNPs), private SNPs (not defining haplogroups), and low-frequency heteroplasmy SNPs across the entire mitochondrial genome. The mtDNA sequences were analyzed using HaploGrep (www.haplogrep.uibk.ac.at) to identify the mtDNA haplogroups. SNP variants were verified using www.MitoMap.com, www.Phylotree.org, and/or www.hmtvar.uniba.it

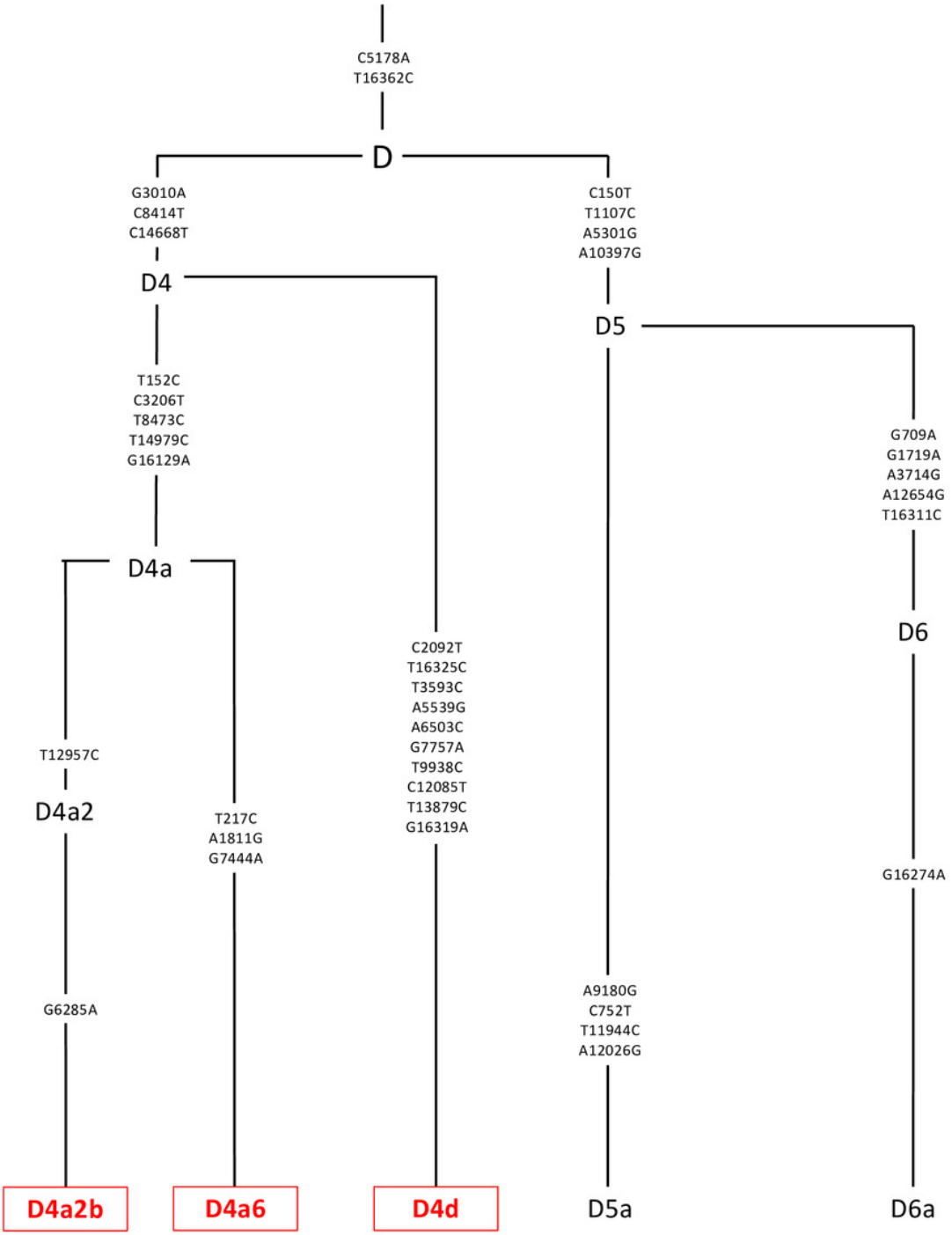
C5178A
T16362C
D
G3010A
C8414T
C14668T
C150T
T1107C
A5301G
A10397G
D4
D5
T152C
C3206T
T8473C
T14979C
G16129A
G709A
G1719A
A3714G
A12654G
T16311C
D4a
D6
C2092T
T16325C
T3593C
A5539G
A6503C
G7757A
T9938C
C12085T
T13879C
G16319A
T12957C
D4a2
T217C
A1811G
G7444A
G16274A
A9180G
C752T
T11944C
A12026G
G6285A
D4a2b
D4a6
D4d
D5a
D6a

Figure 5

L, [A+B], and D untreated cybrids had similar cellular relative metabolic activity.

Cybrid cell lines of the fifth passage, containing mitochondria with either L, [A+B], or D haplogroups, were cultured in flasks until confluent. They were then plated on a 96-well plate with each well containing 50,000 cells and incubated at 37°C for another 48 hours. The MTT assay was then conducted to assess relative cellular metabolic activity. Absorbance was measured on an absorbance reader at 570 nm (measured) and 630 nm (reference). Cybrids had statistically similar relative cellular metabolic activities. (A) All values were normalized to the average of the untreated-L cybrids and displayed as the mean ± Standard Error Margin (SEM). (B) The distribution of each value was also presented in a dot-plot graph representing mean ± Standard Deviation (SD). The untreated-L cybrids (102.4% ± 7.0% SEM; SD = 21.0%, n = 7) had similar relative cellular metabolic activity when compared to the untreated-D cybrids (111.7% ± 4.3% SEM; SD = 11.3%, n = 3, p = 0.311) and the untreated-[A+B] cybrids (95.0% ± 8.5% SEM; SD = 20.9%, n = 4, p = 0.512). Untreated-[A+B] cybrids showed similar cellular metabolic activity compared to the untreated-D cybrids (p = 0.0933). Experiments were analyzed in quadruplicate, and the entire experiment was repeated twice. *$p < 0.05$; **$p < 0.01$; ***$p < 0.001$.

A

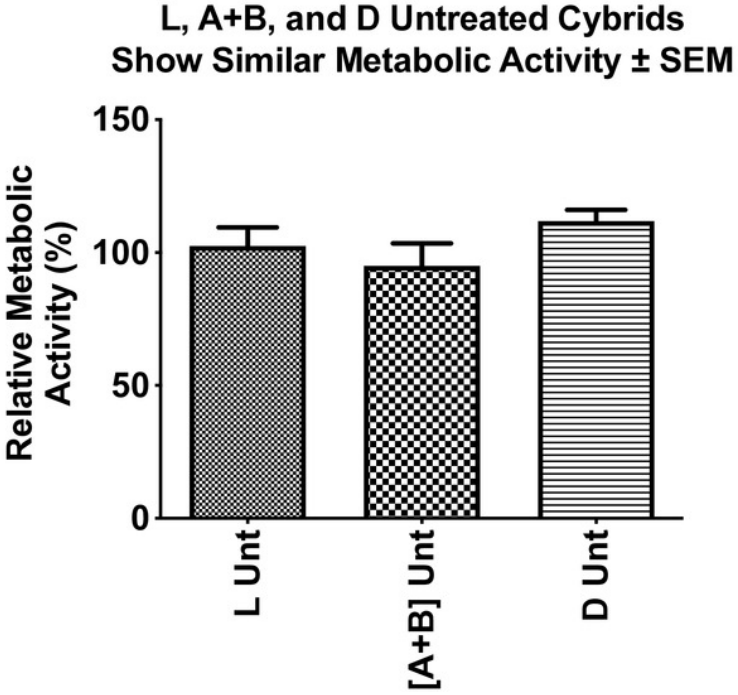
L, A+B, and D Untreated Cybrids
Show Similar Metabolic Activity ± SEM
Relative Metabolic Activity (%)
150
100
50
0
L Unt
[A+B] Unt
D Unt

B

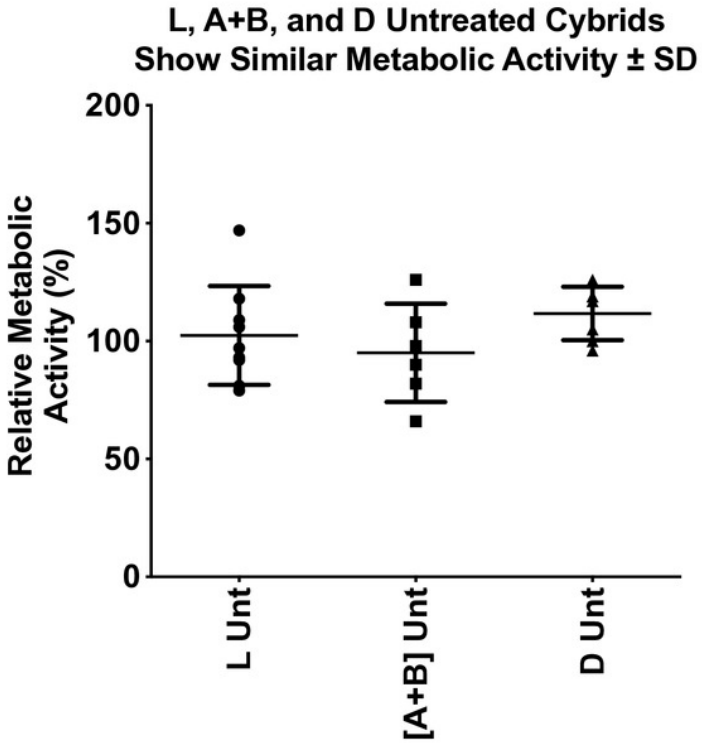
L, A+B, and D Untreated Cybrids
Show Similar Metabolic Activity ± SD
Relative Metabolic Activity (%)
200
150
100
50
0
L Unt
[A+B] Unt
D Unt

Figure 6

L, [A+B], and D cybrids vary in relative cellular metabolic activity after cisplatin treatment.

L, [A+B], and D cybrids in the fifth passage were cultured and then plated on 96-well plates with each well containing 50,000 cells. After 24 hours, media were removed, and cells were treated with 100 µL of 40 µM concentration of cisplatin. Plates were then incubated at 37° C for another 48 hours. The MTT assay was conducted to assess relative cellular metabolic activity. Absorbance values were measured on an absorbance reader at 570 nm (measured) and 630 nm (reference). (A) All values were normalized to the average of the untreated-L cybrids and displayed as the mean ± Standard Error Margin (SEM). (B) The distribution of each value was also presented in a dot-plot graph representing mean ± Standard Deviation (SD). The cisplatin-treated-L cybrids showed the greatest reduction in relative cellular metabolic activity compared to the untreated-L cybrids (75.0% ± 6.7% SEM; SD = 20.0%, n = 7; 102.4% ± 7.0% SEM; SD = 21.0%, n = 7, respectively) ($p = 0.0117$). The cisplatin-treated-D cybrids showed a significant decrease in cell viability compared to the untreated-D cybrids (86.9% ± 1.6% SEM; SD = 4.3%, n = 3; 111.7% ± 4.3% SEM; SD = 11.3%, n = 3, respectively) ($p = 0.0001$). The cisplatin-treated-[A+B] cybrids also had a statistically significant decrease in cellular metabolic activity compared to their respective untreated-[A+B] cybrids (70.3% ± 4.5% SEM; SD = 11.1%, n = 4; 95.0% ± 8.5% SEM; SD = 20.9%, n = 4, respectively) ($p = 0.0285$). Each treatment was run in quadruplicate and the entire experiment was repeated twice. *$p < 0.05$; **$p < 0.01$; ***$p < 0.001$.

A

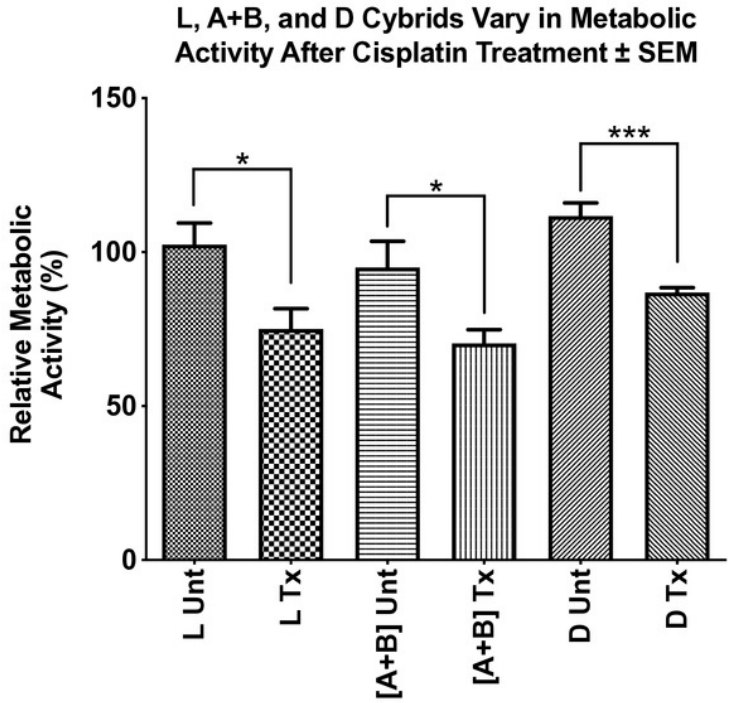
L, A+B, and D Cybrids Vary in Metabolic Activity After Cisplatin Treatment ± SEM
Relative Metabolic Activity (%)
150
100
50
0
*
*
***
L Unt
L Tx
[A+B] Unt
[A+B] Tx
D Unt
D Tx

B

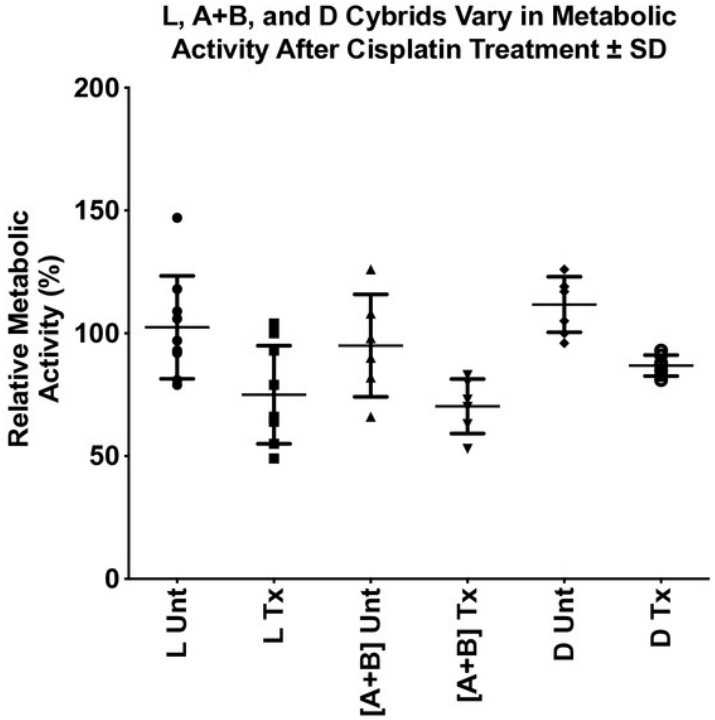
L, A+B, and D Cybrids Vary in Metabolic Activity After Cisplatin Treatment ± SD
Relative Metabolic Activity (%)
200
150
100
50
0
L Unt
L Tx
[A+B] Unt
[A+B] Tx
D Unt
D Tx

Figure 7

L, [A+B], and D cybrids maintained mitochondrial membrane potential (ΔΨm) after cisplatin treatment.

Mitochondrial Membrane Potentials for untreated and treated cybrid cells were measured. Mitochondrial Membrane Potentials for untreated and treated cybrid cells were measured. L, [A+B], and D cybrids were cultured to the fifth passage and then plated in 24-well plates (100,000 cells/well), incubated 24 hours and treated with 0 or 40μM of cisplatin for another 48 hours. The JC-1 assay was conducted and fluorescence values were obtained using a microplate reader. All values were normalized to the average of the untreated-L cybrids. (A) All values were normalized to the average of the untreated-L cybrids and displayed as the mean ± Standard Error Margin (SEM). (B) The distribution of each value was also presented in a dot-plot graph representing mean ± Standard Deviation (SD). Results indicated that there was no significant difference in mitochondrial membrane potential after cisplatin treatment in L, [A+B], or D cybrids. Cisplatin-treated-L cybrids had a relative mitochondrial membrane potential of 108.4% ± 8.2% SEM; SD = 21.8% versus untreated-L cybrids (101.0% ± 11.2% SEM; SD = 29.5%, n = 7, p = 0.602). Cisplatin-treated-[A+B] displayed 136.5% ± 33.9% SEM; SD = 67.8% versus untreated-[A+B] cybrids (147.5% ± 42.0% SEM; SD = 84.0%, n = 4, p = 0.845). The cisplatin-treated-D cybrids were observed to have a relative mitochondrial membrane potential of 115.0% ± 3.5% SEM; SD = 7.0% versus the untreated-D cybrids (127.3% ± 20.1% SEM; SD = 40.3%, n = 4, p = 0.571) (*Fig. 7A*). Each treatment was run in quadruplicate and the entire experiment was repeated twice. $p < 0.05$; $^{**}p < 0.01$; $^{***}p < 0.001$.

A

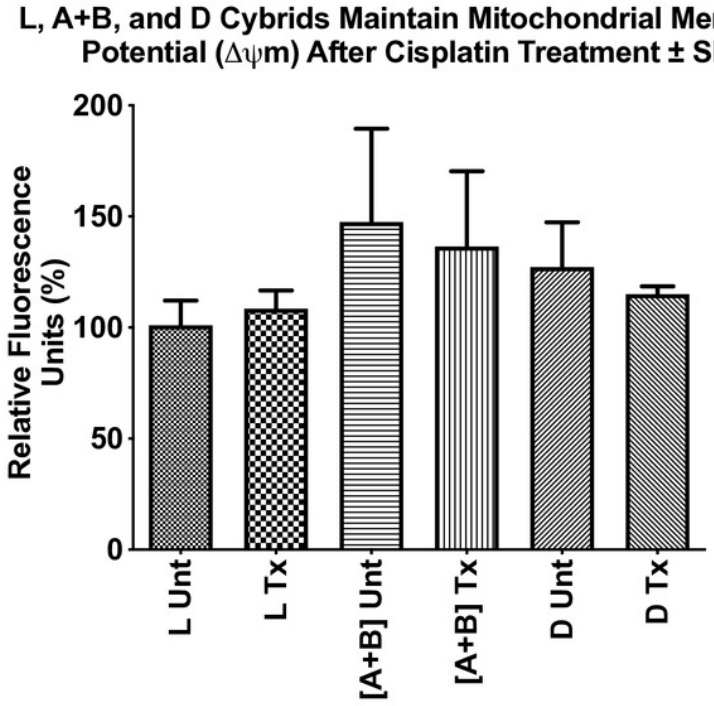
L, A+B, and D Cybrids Maintain Mitochondrial Membrane Potential (Δψm) After Cisplatin Treatment ± SEM
Relative Fluorescence Units (%)
200
150
100
50
0
L Unt
L Tx
[A+B] Unt
[A+B] Tx
D Unt
D Tx

B

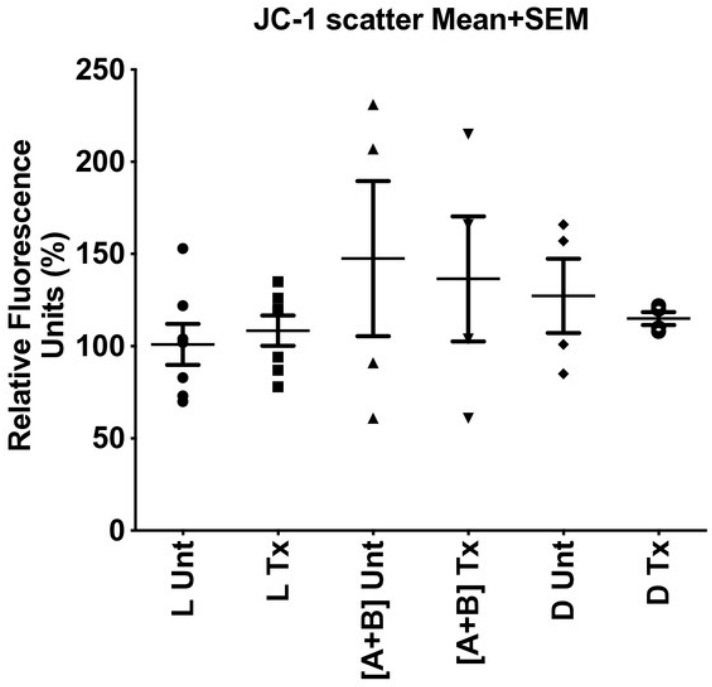
JC-1 scatter Mean+SEM
Relative Fluorescence Units (%)
250
200
150
100
50
0
L Unt
L Tx
[A+B] Unt
[A+B] Tx
D Unt
D Tx

Figure 8

ARPE-19 Cells maintained mitochondrial membrane potential (ΔΨm) after cisplatin treatment (Incucyte® Live Cell Analyzer).

After cisplatin treatment, the cybrids showed decreased metabolic activity but the mitochondrial membrane potentials remained unchanged, which was unexpected. Therefore, we conducted additional experiments using the ARPE-19 cell line that allowed for comparison of growth/proliferation over 40 hours in cultures treated with 20 µM or 40 µM cisplatin (n = 7 per treatment condition). The mitochondrial membrane potential was measured with the JC-1 reagent that was added to cultures for 15 minutes. Fluorescence was measured for red and green wavelengths using a microplate reader. (A) All values were displayed as the mean ± SD. Over the first 8 hours of culture, the untreated and cisplatin-treated ARPE-19 cells showed similar rates of growth. (B) By 10 hours the untreated ARPE-19 cells showed an increasing slope of growth compared to the 20 µM and 40 µM cultures that were stagnant in their growth. By 40 hours, the untreated had a 2-fold higher number of cells than cisplatin-treated cultures. (Untreated 1969 ± 115 standard deviation (SD)), versus 20 µM (1023 ± 81 SD, $p = 0.0006$) and 40 µM (945 ± 74 SD, $p = 0.0001$) (At 40 hours, the ΔΨm levels were similar between the untreated AREP-19 (1.8993 ± 0.145 SD) versus 20 µM (2.0698 ± 0.161 SD, p = NS) and 40 µM (2.0520 ± 0.162 SD, p = NS) cisplatin-treated ARPE-19 cultures. $p < 0.05$; $**p < 0.01$; $***p < 0.001$.

A

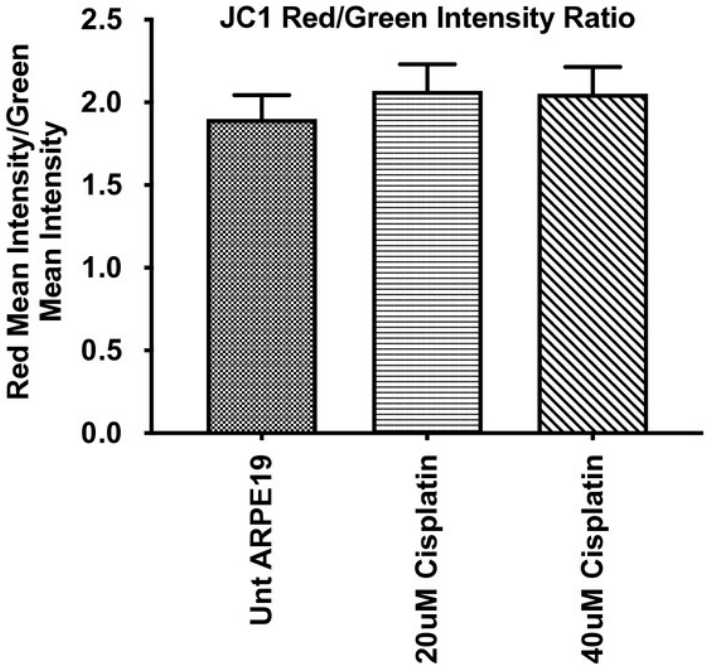
JC1 Red/Green Intensity Ratio
Red Mean Intensity/Green Mean Intensity
2.5
2.0
1.5
1.0
0.5
0.0
Unt ARPE19
20uM Cisplatin
40uM Cisplatin

B

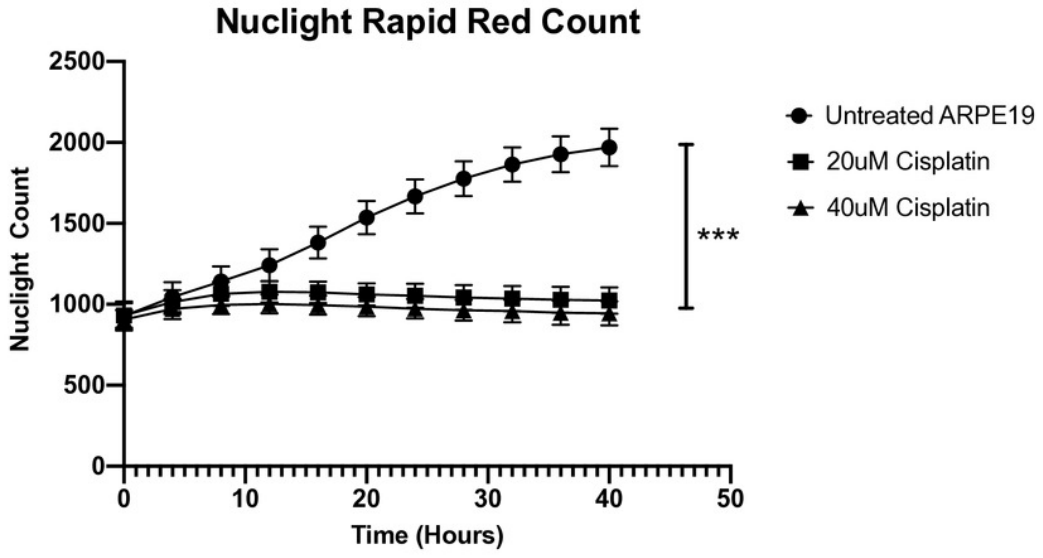
Nuclight Rapid Red Count
Nuclight Count
2500
2000
1500
1000
500
0
0
10
20
30
40
50
Time (Hours)
***
Untreated ARPE19
20uM Cisplatin
40uM Cisplatin

Figure 9

L, [A+B], and D cybrids vary in LDH cytotoxicity.

The cytotoxicity levels of L, [A+B], and D cybrids were measured with the lactate dehydrogenase (LDH) assay. Cybrids cultured to the fifth passage were plated in 96-well plates (10,000 cells/ well) for 24 hours and treated with 0 or 40μM of cisplatin for another 48 hours. The LDH assay was conducted and absorbance values were taken at both 490 nm and 680 nm using an absorbance reader. Percent cytotoxicity levels were calculated using the equation (Treated LDH level – spontaneous LDH level) divided by (Maximum LDH level – spontaneous LDH level) multiplied by one hundred. (A) All values were normalized to the average of the untreated-L cybrids and displayed as the mean ± Standard Error Margin (SEM). (B) The distribution of each value was also presented in a dot-plot graph representing mean ± Standard Deviation (SD). When normalized to the L cybrids, there were significantly higher LDH cytotoxicity levels in L cybrids compared to [A+B] cybrids (111.5% ± 16.5% SEM; SD = 40.5%, n = 6 versus 41.8% ± 9.8% SEM; SD = 16.9%, n = 3, respectively) ($p = 0.0270$). The D cybrids trended lower LDH levels but they were not significant (48.9% ± 20.2% SEM; SD = 35.0%, n = 3, $p = 0.0576$) compared to the L cybrids. LDH cytotoxicity levels between the [A+B] and D cybrids were not statistically different ($p = 0.766$). The entire experiment was repeated three separate times. *$p < 0.05$; **$p < 0.01$; ***$p < 0.001$.

A

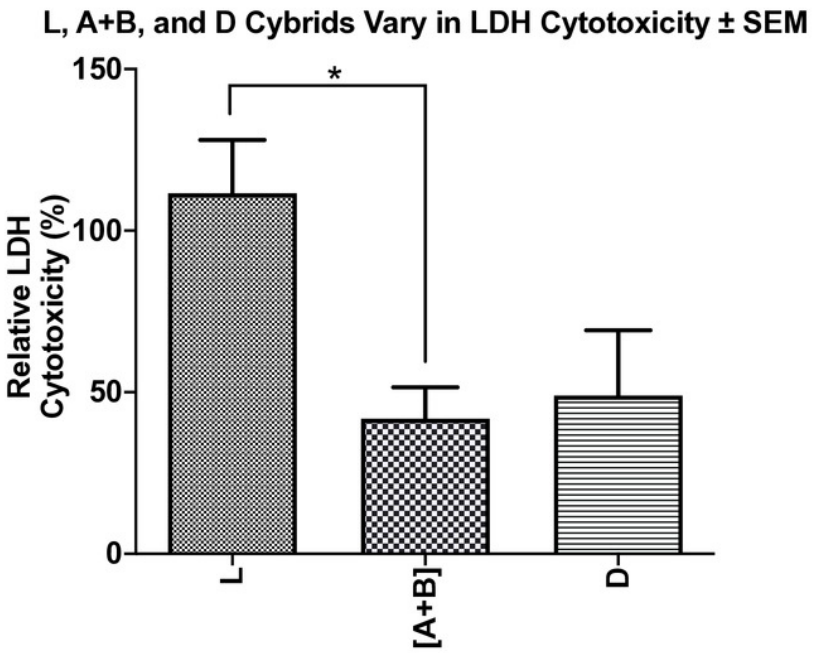
L, A+B, and D Cybrids Vary in LDH Cytotoxicity ± SEM
Relative LDH Cytotoxicity (%)
150
100
50
0
*
L
[A+B]
D

B

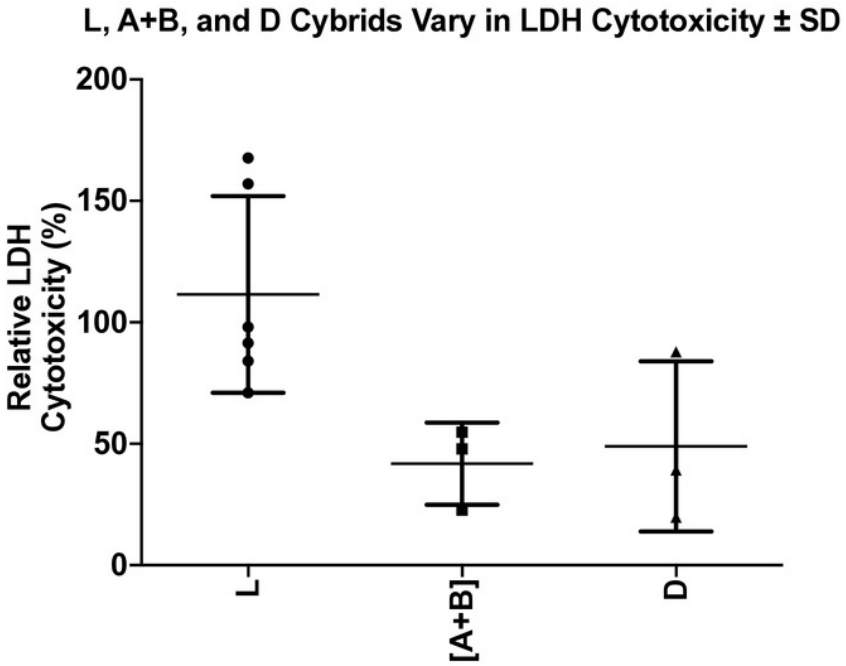
L, A+B, and D Cybrids Vary in LDH Cytotoxicity ± SD
Relative LDH Cytotoxicity (%)
200
150
100
50
0
L
[A+B]
D

Table 1(on next page)

Haplogroup profiles for the ARPE-19 cybrids.

Illustration of cybrid cell lines used with their associated haplogroup type along with the age and gender of the respective donor. Cytoplasmic hybrids (cybrids), cell lines with identical nuclear genomes but different mitochondrial genomes, were created and used in the fifth passage for all experiments. Cybrid cells were created using platelets isolated from peripheral blood that was fused with Rho0 (mtDNA free) ARPE-19 cells. The mtDNA haplogroups for each subject and cybrid cell line were identified using polymerase chain reaction (PCR) along with restriction enzyme digestion and mtDNA sequencing. DNA was extracted from the individual cybrids (n = 7 for L cybrids, n = 4 for [A+B] cybrids, and n = 3 for D cybrids) using a kit. Next Generation Sequencing (NGS) technology was used to sequence both strands of mtDNA independently in both directions. This was done to quantitate the haplogroup-defining single nucleotide polymorphisms (SNPs), private SNPs (not defining haplogroups), and low-frequency heteroplasmy SNPs across the entire mitochondrial genome. All of the SNPs identified had a Quality Score of 100 and Passed all of the Filters.

1

Subject	Haplogroup	Age	Gender
Cyb L 11-38	L0a1a1	38	F
Cyb L 11-30	L1b1a	54	F
Cyb L 13-126	L1b1a7	39	F
Cyb L 13-124	L1b2a	31	M
Cyb L 13-125	L1c2a1	52	F
Cyb L 11-31	L2b2	42	M
Cyb L 11-17	L3e1a1a	64	F
Cyb A 11-16	A2	42	F
Cyb A 11-14	A2w	34	F
Cyb B 12-40	B	31	M
Cyb B 13-68	B2a	45	F
Cyb D 13-55	D4a2b	45	F
Cyb D 11-18	D4a6	39	M
Cyb D 11-29	D4d	37	F

Table 2(on next page)

L, A+B, and D mtDNA haplogroup ARPE-19 cybrids displayed unique SNP variants.

SNP Variants associated with the L, [A+B], and D mtDNA haplogroups were compared to one another. Nucleotide changes containing one or more differences between the studied haplogroups were identified and analyzed. The location of the nucleotide change within the mtDNA, the base pair changed, their associated rs number, their presence in the L, [A+B], or D cybrids, and any associated pathogenesis found in the literature were identified and displayed. Non-synonymous changes present in some but not all haplogroups tested were found at 4824 A>G, rs ND; 5178 C>A, rs28357984; 5442 T>C, rs3020601; 7146 G>A, rs372136420; 8701 G>A, rs2000975; 8794 C>T , rs2298007; 10398 G>A, rs2853826; and 13105 G>A, rs2853501. Data was incorporated using www.hmtvar.uniba.it as well as www.phylotree.org.

1
2

Loci: MT-	SNP	AA Change	rs#	Present in L Cybrids	Present in A+B Cybrids	Present in D Cybrids	Related Pathogenesis
D-Loop	152 C>T	Noncoding	rs117135796	No	Yes	Yes	Predisposition to ataxia, bladder cancer, aging, hepatocellular carcinoma, predisposition to breast cancer, lung cancer, nasopharyngeal carcinoma, stomach cancer, liver cancer, ovarian carcinoma
D-Loop	182 T>C	Noncoding	rs41473347	No	Yes	Yes	Predisposition to ataxia, bladder cancer, lung cancer
D-Loop	195 C>T	Noncoding	rs2857291	No	Yes	Yes	Bipolar disease, predisposition to ataxia, bladder cancer, aging, breast cancer, lung cancer
D-Loop	235 A>G	Noncoding	rs3937037	No	Yes	No	Lung cancer
D-Loop	247 A>G	Noncoding	rs41334645	No	Yes	Yes	Predisposition to ataxia
D-Loop	263 G>A	Noncoding	rs2853515	Yes	No	No	Oncocytic adenomas, predisposition to ataxia, breast cancer, nasopharyngeal carcinoma
RNR1	663 A>G	rRNA	ND	No	Yes	No	Hearing loss
RNR1	769 A>G	rRNA	rs2853519	No	Yes	Yes	N/A
RNR1	825 A>T	rRNA	rs2853520	No	Yes	Yes	N/A
RNR1	1018 A>G	rRNA	rs2856982	No	Yes	Yes	Heteroplasmic variant
RNR1	1048 C>T	rRNA	rs2000974	Yes	No	No	Heteroplasmic variant, hearing loss

RNR2	1736 A>G	rRNA	rs193303006	No	Yes	No	Heteroplasmic variant
RNR2	2758 A>G	rRNA	rs2856980	No	Yes	Yes	N/A
RNR2	2885 C>T	rRNA	rs2854130	No	Yes	Yes	N/A
ND1	3516 C>A	syn:L-L	rs2854132	Yes	No	No	N/A
ND1	3594 T>C	syn:V-V	rs193303025	No	Yes	Yes	Thyroid tumor
ND1	4104 G>A	syn:L-L	rs1117205	No	Yes	Yes	N/A
ND1	4248 T>C	syn:I-I	rs9326618	No	Yes	No	Homoplasmic variant
ND2	4824 A>G	**non-syn:T-A**	ND	**No**	**Yes**	**No**	Glaucoma
ND2	5178 C>A	**non-syn:L-M**	rs28357984	**No**	**No**	**Yes**	Infertility, increased longevity, diabetes, atherosclerosis, hypertension, myocardial infarction, Parkinson's disease, glaucoma, blood iron metabolism, and cardiovascular disease
ND2	5442 T>C	**non-syn:F-L**	rs3020601	**Yes**	**No**	**No**	Risk of mobility impairment
CO1	6185 T>C	syn:F-F	rs1029272	Yes	No	No	Primary Open-Angle Glaucoma (POAG)
CO1	7146 G>A	**non-syn:T-A**	rs372136420	**No**	**Yes**	**Yes**	Asthenospermia
CO1	7256 T>C	syn:N-N	ND	No	Yes	Yes	N/A
TD	7521 A>G	tRNA	rs200336937	No	Yes	Yes	Thyroid cancer, colorectal tumor
ATP8	8468 T>C	syn:L-L	rs1116907	No	Yes	Yes	N/A
ATP6	8655 T>C	syn:I-I	rs2853822	No	Yes	Yes	N/A
ATP6	8701 G>A	**non-syn:T-A**	rs2000975	**No**	**Yes**	**No**	Neuromuscular disorders, somatic lung cancer, thyroid cancer, fertilization

							failure, atherosclerosis, irritable bowel syndrome, osteosarcoma, MELAS, cardiomyopathy, Parkinson disease, hearing loss
ATP6	8794 C>T	**non-syn:H-Y**	rs2298007	**No**	**Yes**	**No**	Homoplasmic variant, coronary arteriosclerosis, irritable bowel syndrome
ATP6	9042 C>T	syn:H-H	rs3020605	Yes	No	No	Homoplasmic variant
CO3	9347 A>G	syn:L-L	rs2853824	Yes	No	No	Homoplasmic variant
CO3	9540 C>T	syn:L-L	rs2248727	No	Yes	No	Normal-Tension Glaucoma (NTG)
ND3	10398 G>A	**non-syn:T-A**	rs2853826	**No**	**Yes**	**No**	IVF failure, Fuch's Endothelial Corneal Dystrophy (FECD), breast cancer, esophageal cancer, aging, diabetes, osteoarthritis, schizophrenia, LHON
ND4L	10589 G>A	syn:L-L	rs2853487	Yes	No	No	Homoplasmic variant
ND4L	10688 A>G	syn:V-V	rs2853488	No	Yes	Yes	N/A
ND4	10810 C>T	syn:L-L	rs28358282	No	Yes	Yes	N/A
ND4	10873 C>T	syn:P-P	rs2857284	No	Yes	No	Ischemic stroke
ND4	12007 G>A	syn:W-W	rs2853497	Yes	No	No	Homoplasmic variant
ND5	12705 T>C	syn:I-I	rs193302956	No	Yes	No	Neuropathy, dystonia, myoclonic epilepsy, MERRF, PD, schizophrenia, bipolar disorder, infantile cardiomyopathy, diabetes, hypertension, AD,

							Leigh syndrome, blood pressure
ND5	12720 A>G	syn:M-M	rs2853500	Yes	No	No	Homoplasmic variant
ND5	13105 G>A	**non-syn:I-V**	s2853501	**No**	**Yes**	**Yes**	Deafness, neuropathy
ND5	13506 T>C	syn:Y-Y	rs2857287	No	Yes	Yes	N/A
ND5	13650 T>C	syn:P-P	rs2854123	No	Yes	Yes	N/A
CYB	15301 A>G	syn:L-L	rs193302991	No	Yes	No	Homoplasmic variant
CYB	15301 G>A	syn:L-L	rs193302991	No	Yes	Yes	Homoplasmic variant
D-Loop	16129 A>G	Noncoding	rs41534744	No	Yes	Yes	Ewing's sarcoma, predisposition to breast cancer, nasopharyngeal carcinoma
D-Loop	16187 T>C	Noncoding	ND	No	Yes	Yes	Friedreich's ataxia, bladder cancer, lung cancer
D-Loop	16189 T>C	Noncoding	rs28693675	No	Yes	No	Diabetes mellitus, insulin resistance, cardiomyopathy, hypertension, Friedreich's ataxia, Ewing's sarcoma, obesity, predisposition to breast cancer, nasopharyngeal carcinoma
D-Loop	16189 C>T	Noncoding	rs28693675	No	Yes	Yes	Diabetes mellitus, insulin resistance, cardiomyopathy, hypertension, Friedreich's ataxia, Ewing's sarcoma, obesity, predisposition to breast cancer, nasopharyngeal carcinoma
D-Loop	16223 T>C	Noncoding	rs2853513	No	Yes	No	Mitochondrial disease , predisposition to

							ataxia, bladder cancer, predisposition to breast cancer, lung cancer, nasopharyngeal carcinoma, stomach cancer, liver cancer
D-Loop	16278 T>C	Noncoding	rs41458645	No	Yes	Yes	Bladder cancer, predisposition to breast cancer, lung cancer
D-Loop	16290 C>T	Noncoding	ND	No	Yes	No	Parkinson's disease
D-Loop	16311 C>T	Noncoding	rs34799580	No	Yes	Yes	Bladder cancer, predisposition to breast cancer, lung cancer
D-Loop	16319 G>A	Noncoding	rs35105996	No	Yes	No	Homoplasmic variant
D-Loop	16362 T>C	Noncoding	rs62581341	No	No	Yes	Homoplasmic variant, mitochondrial disease, bladder cancer , predisposition to breast cancer, lung cancer, stomach cancer, liver cancer

ND, Not Determined

All SNP's had a Quality (A Phred-scaled quality score assigned by the variant caller) Score of 100 and Passed all the Filters.

Table 3(on next page)

L, [A+B], and D mtDNA haplogroup cybrids each displayed unique overall results in cell and gene expression studies.

Results from the cell and gene expression studies were congregated into one table. As illustrated, each haplogroup had a unique result when observed in large as a summation of the assays and gene expression results. As demonstrated from the cell and gene expression studies, L cybrids had decreased cellular metabolic activity and *ALK* gene expression after cisplatin treatment ($p = 0.0117$, $p < 0.0001$ respectively). [A+B] cybrids had decreased cellular metabolic activity, *ALK* gene expression, and *EGFR* gene expression after cisplatin treatment ($p = 0.0285$, $p = 0.0001$, $p = 0.0246$, respectively). D cybrids had decreased cellular metabolic activity after cisplatin treatment ($p = 0.0001$). *$p < 0.05$; **$p < 0.01$; ***$p < 0.001$.

1

	Haplogroup		
	L	**[A+B]**	**D**
Untreated vs. Cisplatin Treated			
Cell Viability	↓ *	↓ *	↓ ***
Mitochondrial Membrane Potential	—	—	—
LDH Cytotoxicity	L — * — [A+B] — NS — D L — NS — D		
Gene Expression Untreated to Treated			
ALK	↓ ****	↓ ***	—
BRAC1	—	—	—
EGFR	—	↓ *	—
ERBB2/ HER2	—	—	—

Table 4(on next page)

L, [A+B], and D mtDNA haplogroup cybrids had varying gene expression values after treatment with cisplatin.

Gene expression results, as well as detailed overviews for*ALK,BRCA1,EGFR, andERBB2/HER2*genes, were summarized into one table. Gene expression values were observed with qPCR for all L, [A+B], and D cybrids and assessed for statistical significance relative to their untreated controls. Cybrids cultured to the fifth passage were plated in six-well plates (500,000 cells/well) and incubated for 24 hours. Cybrids were then treated with culture media containing either 0 or 40μM of cisplatin for an additional 48 hours. RNA was isolated and qRT-PCR was conducted to analyze gene expression. Cancer-related nuclear genes were selected as they are common targets and biomarkers in chemotherapeutic treatments. Fold differences were quantified using the equation 2(ΔΔCt), and the values for each sample were normalized to that of the untreated for each haplogroup. There were significant drops in gene expression levels in the treated-L cybrids for*ALK*gene expression (-18.8% ± 9.7%, $p < 0.0001$), and treated-[A+B] for both*ALK*and*EGFR*gene expression levels (-17.5% ± 9.5%, $p = 0.0001$; -49.2% ± 17.1%, $p = 0.025$). Each experiment was conducted three separate times. *$p < 0.05$; **$p < 0.01$; ***$p < 0.001$.

SYMBOL	GENE NAME	GENBANK ACCESSION NUMBERS	FUNCTIONS	L Cybrids Untreated# vs Treated P value, Fold	[A+B] Cybrids Untreated # vs Treated P value, Fold	D Cybrids Untreated# vs Treated P value, Fold
ALK	Anaplastic Lymphoma Receptor Tyrosine Kinase	NM_004304	Receptor tyrosine kinase that plays an important role in the development of the brain. Found to be rearranged, mutated, or amplified in a series of tumors resulting in many types of cancers.	**<0.0001****, **0.188 ± 0.0973**	**0.0001***, **0.175 ± 0.0950**	0.290, 2.82 ± 1.48
BRCA1	DNA Repair associated	NM_007294	Nuclear Phospho-protein that acts as a tumor suppressor by maintaining genomic stability. Involved in transcription, DNA, repair of double-stranded breaks, recombination.	0.356, 1.36 ± 0.372	0.294, 1.55 ± 0.477	0.158, 3.42 ± 1.39
EGFR	Epidermal Growth Factor Receptor	NM_005228	Triggers cell proliferation when bound to epidermal growth factor.	0.301, 0.760 ± 0.217	**0.0246*, 0.492 ± 0.171**	0.218, .602 ± 0.273
ERBB2/HER2	Erb-b2 Receptor Tyrosine Kinase 2	NM_004448	Members of epidermal growth factor receptor family of receptor tyrosine kinases. Stabilizes binding of epidermal growth factors to receptor.	0.839, 1.06 ± 0.298	0.379, 0.820 ± 0.189	0.325, 1.96 ± 1.75

1